

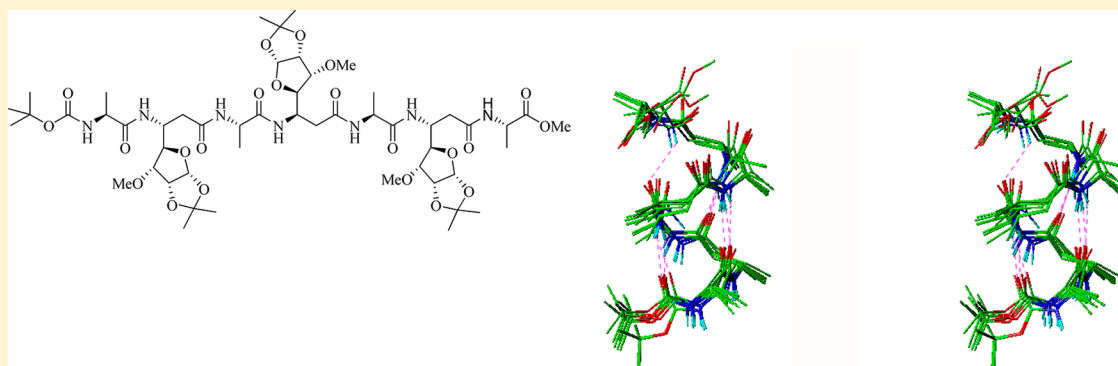
## Design of $\beta$ -Amino Acid with Backbone–Side Chain Interactions: Stabilization of 14/15-Helix in $\alpha/\beta$ -Peptides

Gangavaram V. M. Sharma,<sup>\*,†</sup> Thota Anupama Yadav,<sup>†,‡</sup> Madavi Choudhary,<sup>§,‡</sup> and Ajit C. Kunwar<sup>\*,§</sup>

<sup>†</sup>Organic and Biomolecular Chemistry Division, CSIR-Indian Institute of Chemical Technology, Hyderabad 500 007, India

<sup>§</sup>Centre for Nuclear Magnetic Resonance, CSIR-Indian Institute of Chemical Technology, Hyderabad 500 007, India

**S** Supporting Information



**ABSTRACT:** A new C-linked carbo- $\beta$ -amino acid, (*R*)- $\beta$ -Caa<sub>(r)</sub>, having a carbohydrate side chain with *D*-ribo configuration, was prepared from *D*-glucose by inverting the C-3 stereocenter to introduce constraints/interactions. From the NMR studies it was inferred that the new monomer may participate in additional electrostatic interactions, facilitating and enhancing novel folds in oligomeric peptides derived from it. The  $\alpha/\beta$ -peptides, synthesized from alternating *L*-Ala and (*R*)- $\beta$ -Caa<sub>(r)</sub>, have shown the presence of 14/15-helix by NMR (in CDCl<sub>3</sub>, methanol-*d*<sub>3</sub> and CD<sub>3</sub>CN), CD and MD calculations. The hybrid peptides showed the presence of electrostatic interactions involving the intraresidue amide proton and the C3-OMe, which helped in the stabilization of the NH(*i*)...CO(*i*-4) H-bonds and adoption of 14/15-helix. The importance of such additional interactions has been well defined in recent times to stabilize the folding in a variety of peptidic foldamers. These observations suggest and emphasize that the side chain–backbone interactions are crucial in the stabilization of the desired folding propensity. The designed monomer thus enlarges the opportunities for the synthesis of peptides with novel conformations and expands the repertoire of the foldamers.

### INTRODUCTION

The fascination in understanding the relationship between the structure and function of the proteins<sup>1</sup> has mainly been responsible for the substantial activity in the area of peptidomimetics. The design of a variety of monomers and their oligomers has spawned a novel field of “foldamers”,<sup>2</sup> allowing the creation of several folding patterns that mimic the biopolymers. A large number of such foldamers have been conventionally prepared from subunits or the residues, which are from the same class and thus consist of homogeneous backbones. It was only during the past decade that peptide foldamers derived from heterogeneous backbones,<sup>3</sup> referred to as hybrid peptides, were investigated. The first regular series of such foldamers, the  $\alpha/\beta$ -peptides,<sup>4,5</sup> were designed from the 1:1 arrangement of  $\alpha$ - and  $\beta$ -amino acids. Gellman et al.<sup>5a</sup> in their pioneering studies on the  $\alpha/\beta$ -peptides, derived from *L*-Ala and (*S,S*)-*trans*-2-aminocyclopentanecarboxylic acid (ACPC), found the NMR observations consistent with a rapid equilibrium between 11- and 14/15-helical structures. Such a behavior is well-documented among proteins and peptides containing  $\alpha$ -

amino acid residues exclusively, which frequently populate both  $\alpha$ - and  $3_{10}$ -helical conformations<sup>6</sup> in solution. Jagadeesh et al.,<sup>7</sup> on the other hand, demonstrated simultaneous presence of 11- and 14/15-helical folds, supported by bifurcated H-bonds in  $\alpha/\beta$ -peptides containing *cis*  $\beta$ -furanoid sugar amino acids. In order to distinguish between the two possibilities, Gellman et al.<sup>8a</sup> carried out structural studies using single crystal X-ray diffraction of a large number of  $\alpha/\beta$ -peptides. These studies revealed that the smaller oligomers exhibit 11-helices, while the longer ones prefer to fold as 14/15-helix, a trend observed in the natural peptides and proteins with respect to  $3_{10}$ - and  $\alpha$ -helices. Likewise, Seebach et al.<sup>9</sup> reported  $\alpha/\beta$ -peptides that fold into the right-handed 14/15-helix, due to the cumulative helix inducing effect of the Aib residues on local conformation, rather than the stabilization through H-bonding. Further, Gellman et al.<sup>8d</sup> have also demonstrated the use of a “diblock” motif strategy in designing the inhibitor of protein–protein

Received: May 2, 2012

Published: July 20, 2012

interactions by the chimeric  $\alpha+\beta$ -peptides.<sup>10</sup> In these systems, the  $\alpha/\beta$ -peptide fragment takes a 14/15-helical structure exclusively, probably driven by the  $\alpha$ -helix generated by the  $\alpha$ -peptide fragment,<sup>10a</sup> similar to the concept of “hybrid helix” proposed by us.<sup>11</sup> The distinctive advantage of these  $\alpha/\beta$ -peptides is the possibility for mimicking surface features of one of the interacting proteins due to the presence of  $\alpha$ -amino acids with the natural side chains, while the  $\beta$ -amino acids play a major role in organizing the conformational space.

To the best of our knowledge, the  $\alpha/\beta$ -peptide class of foldamers,<sup>5,7</sup> depicting such interconverting 11- and 14/15-helices, were mostly derived from cyclic  $\beta$ -amino acids (ACPC, and cis  $\beta$ -furanoid sugar amino acids) having restrictions in the backbone dihedral angles. This prompted Gellman et al. to comment that  $\alpha/\beta$ -peptides containing flexible amino acids do not significantly populate these structures, because of the much lower  $\alpha/\beta$ -peptide helical propensity of the unconstrained  $\beta$ -residues compared to the cyclic ones.<sup>8a</sup> Further, it was suggested<sup>8c</sup> that to induce the preference of 11-helix over a 14/15-helix or vice versa it may be necessary to preorganize the  $\beta$ -amino acids by introducing additional constraints/interactions. However, in the design of Seebach with acyclic  $\beta$ -amino acids, the realization of 14/15-helix has been attributed to the restricted conformational space traversed by the  $\alpha$ -amino acid (Aib) residues, which cumulatively direct the induction of a helix.

Our work on the design of “foldamers” to create skeletal and conformational diversity<sup>12</sup> has been mainly centered around C-linked carbo-amino acids (Caa), the unnatural amino acids with carbohydrate side chains,<sup>13</sup> based on the structures of nikkomycins.<sup>14</sup> In our earlier studies, one family of  $\alpha/\beta$ -peptides derived from alternating C-linked (*S*)-carbo- $\beta$ -amino acid **1** [(*S*)- $\beta$ -Caa<sub>(x)</sub>; with *D*-xylose side chain] (Figure 1) and *L*-

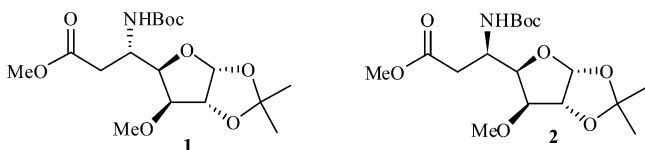


Figure 1. Structures of (*S*)- $\beta$ -Caa<sub>(x)</sub> **1** and (*R*)- $\beta$ -Caa<sub>(x)</sub> **2**.

Ala residues generated novel right-handed 11/9-mixed helix.<sup>15,16</sup> Though the oligomers derived from “epimeric” (at the amine stereocenter) (*R*)- $\beta$ -Caa<sub>(x)</sub> **2** and *D*-Ala in alternation showed the presence of a structure from NMR and CD spectra, it was not possible to identify the folding propensity conclusively. The above results fully endorse the distinctly different behavior of “epimeric” esters **1** and **2** (Figure 1) in their ability to induce the structure.

A literature survey<sup>17</sup> indicated that the interactions with a side chain can be used as additional constraints for the stabilization of secondary structures. In our recent study on  $\alpha/\beta$ -peptides<sup>18</sup> derived from alternating pyran- $\beta$ -amino acid and *L*-Ala, the additional electrostatic interaction between pyran “oxygen” and the preceding NH assisted it to fold into a new 9/11-helix. Furthermore, studies on  $\beta^{2,2}$ -peptides<sup>19</sup> indicated the stabilization of strand structures by an additional electrostatic interaction between the backbone amide proton and oxygen of OMe group at the C-3 of side chain. This result is similar to the evidence found in the literature for S/T turns.<sup>17</sup>

These observations and the knowledge that side chains modulate the folding propensities of the oligomers prompted

us to take up detailed studies on **1** and **2**. NMR studies revealed the presence of a fairly constrained sugar side chain in **2**.  $^3J_{\text{NH-C}\beta\text{H}} = 9.5$  Hz in **2**, implies an *anti*-periplanar arrangement of these protons with  $\phi \approx -120^\circ$ , while,  $^3J_{\text{C}_4\text{H-C}\beta\text{H}} \approx 8.0$  Hz suggests restricted rotation along C $\beta$ -C $_4$  bond with high propensity of *trans* disposition of these protons (Figure 2).

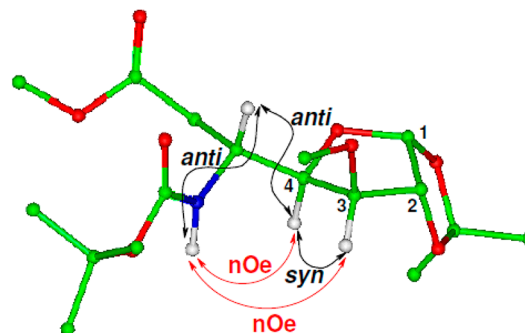


Figure 2. Structure of (*R*)- $\beta$ -Caa<sub>(x)</sub> **2** gleaned from the NMR data.

Thus, the close proximity of NH and C $_4$ H in space is confirmed by strong NOE correlation between them. Incidentally, the presence of C $_3$ H/NH NOE correlation also implies the proximity of these two protons (Figure 2). High propensity to take a single conformation in **2** was revealing.

The above findings on **2** and the requirement for additional constraints/interactions, prompted us to design a new  $\beta$ -amino acid, (*R*)- $\beta$ -Caa<sub>(r)</sub> **3**, with a *D*-ribo side chain, by the inversion of configuration at the C3 of *D*-xylo side chain. Thus in **3**, there is a likelihood of the oxygen of the C-3 OMe coming closer to the NH, if the structural behavior of the sugar ring and the backbone is not altered appreciably from that of **2**. It is presumed that such proximity of NH with oxygen at C-3 in **3** might contribute an additional electrostatic interaction. This in turn may induce a definite fold in the oligomers derived from (*R*)- $\beta$ -Caa<sub>(r)</sub> **3**. To investigate the above concept, in continuation of our work on the design of  $\alpha/\beta$ -peptides,<sup>20</sup> herein we report the synthesis of  $\alpha/\beta$ -peptides **5–9**<sup>21</sup> (Figure 3) containing (*R*)- $\beta$ -Caa<sub>(r)</sub> **3** and *L*-Ala **4** alternately and their structural analysis by NMR, CD and MD studies.

## RESULTS AND DISCUSSIONS

**Synthesis of  $\beta$ -Amino Acid.** The new  $\beta$ -amino acid derivative **3** was prepared from the known ulose derivative<sup>22</sup> of *D*-(+)-glucose (Scheme 1). Accordingly, reduction of **11**, prepared by Swern oxidation of **10**, with NaBH $_4$  in aq. ethanol at 0 °C for 1 h gave **12** (77%), which on subsequent alkylation in 1,4-dioxane with MeI in the presence of KOH for 12 h afforded the methyl ether **13** (80%). Acid hydrolysis of 5,6-acetonide **13** in 60% aq. AcOH furnished the diol **14** (85%), which on oxidative cleavage with NaIO $_4$  gave the aldehyde **14a**.

Subsequently, Wittig olefination of **14a** in CH $_2$ Cl $_2$  for 4 h furnished the ester **15** (84%), which on aza-Michael addition with benzyl amine for 12 h afforded the diastereomers **16** and **17** in 85:15 ratio (66%). After the separation of **16** (27%) and **17** (6%) by column chromatography, ester **16** on reaction with 10% Pd/C–H $_2$  in MeOH at room temperature for 12 h gave the amine **18**, which on further reaction with (Boc) $_2$ O and Et $_3$ N in CH $_2$ Cl $_2$  at 0 °C to room temperature for 2 h furnished **3** in 60% yield. Similarly, catalytic debenzoylation of **17** followed

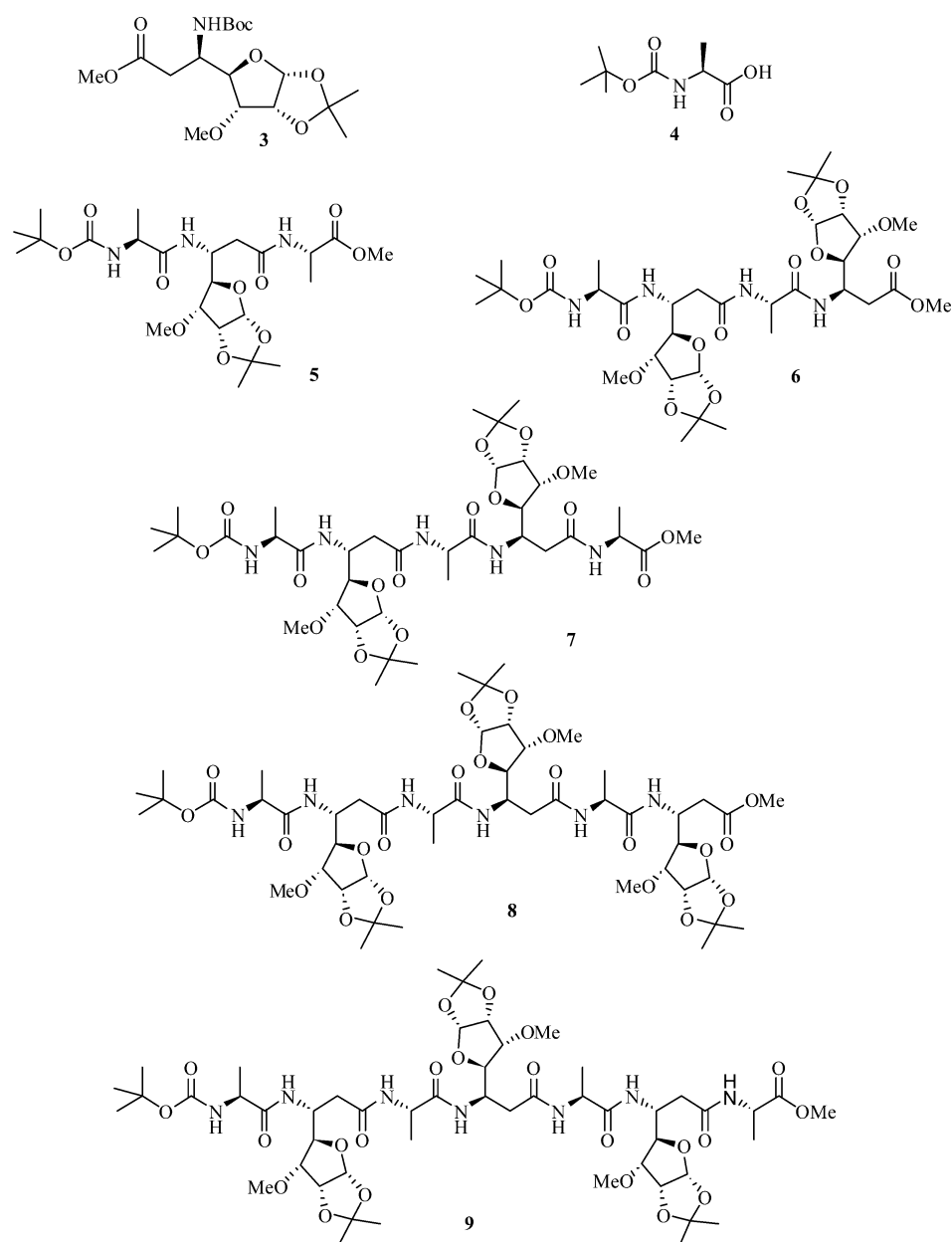


**Figure 3.** Structures of monomers 3, 4 and peptides 5–9.

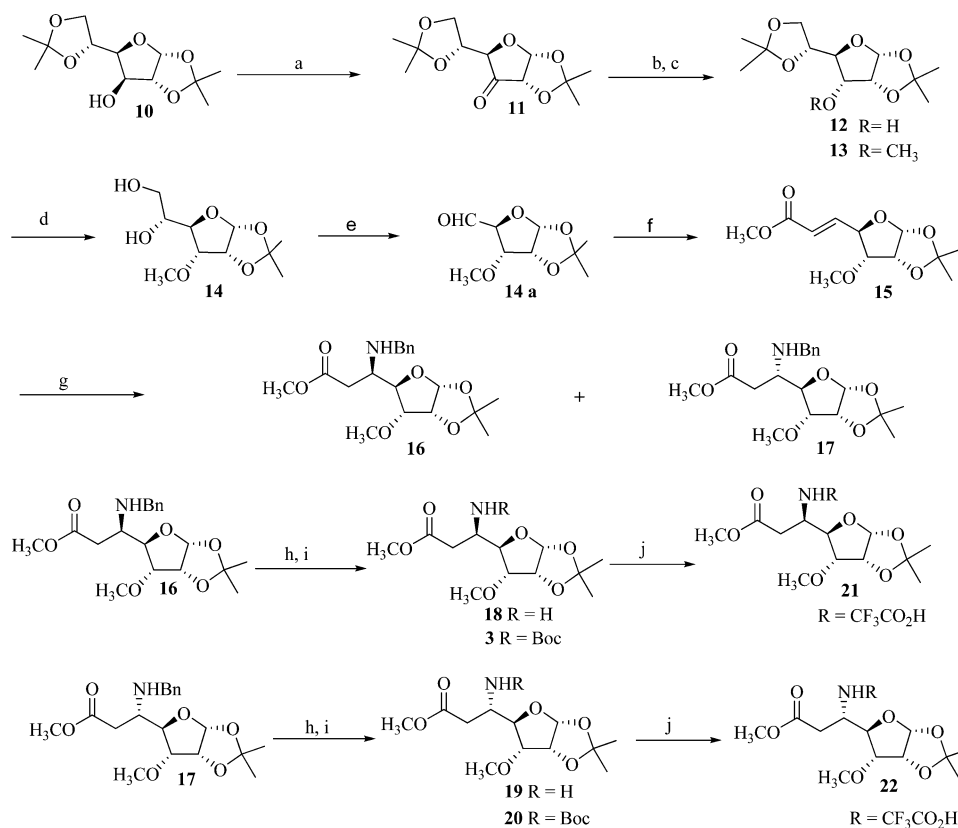
by treatment of the amine **19** with  $(\text{Boc})_2\text{O}$  afforded the (*S*)- $\beta$ -amino acid **20** (60%).

The stereochemistry at the amine center in **16** and **17** was determined by Mosher method,<sup>23</sup> whose details are described in the Supporting Information.<sup>24</sup> Accordingly, the salts **21** and **22**, prepared from the respective esters **3** and **20**, on reaction with (*R*)- and (*S*)-Mosher acids in the presence of EDCI and HOBT in  $\text{CH}_2\text{Cl}_2$  afforded the Mosher amides **23** (77%)/**24** (65%) and **25** (67%)/**26** (61%), respectively<sup>24</sup> (Scheme 2).

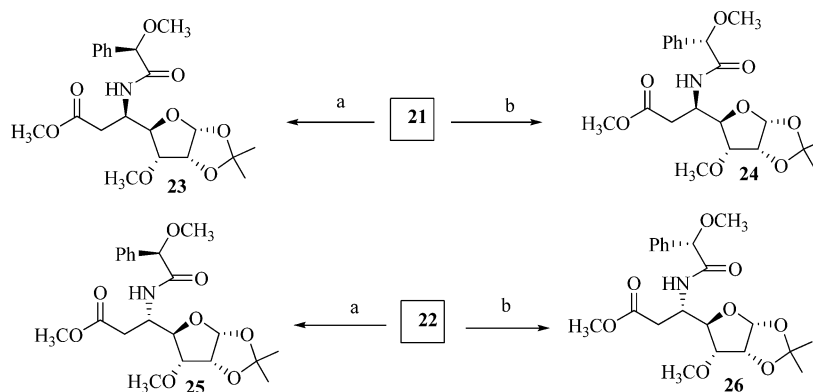
Detailed  $^1\text{H}$  NMR studies (Figure 4) on **3** indicated a fairly constrained carbohydrate side chain resulting in close proximity of the amide proton with  $-\text{OMe}$  oxygen of the sugar ring.  $^3J_{\text{NH-C}\beta\text{H}} = 9.4$  Hz indicated an *anti*-periplanar arrangement of these protons with  $\phi \approx -120^\circ$ , while,  $^3J_{\text{C}\alpha\text{H-C}\beta\text{H}} \approx 8.2$  Hz implies restricted rotation along  $\text{C}\beta\text{-C}\alpha$  bond, with high propensity of *trans*-disposition of these protons. In addition  $^3J_{\text{C}\alpha\text{H-C}\beta\text{H}} \approx 8.4$  Hz involving the ring protons indicates their *trans*-orientation, thus placing the methoxy group at a *syn*

disposition with respect to the amide proton to result in possible electrostatic interaction, as shown in Figure 4. These conclusions are adequately supported by strong NOE correlations  $\text{C}\beta\text{H}/\text{C}\alpha\text{H}$  and  $\text{NH}/\text{C}\alpha\text{H}$ .

**Synthesis of Peptides.** Peptides **5–9** were prepared<sup>21</sup> from Boc-L-Ala-OH (**4**) and **3** by standard peptide coupling methods<sup>23</sup> using EDCI, HOBT and DIPEA in solution phase. Accordingly, **21** on condensation with acid **4** (Scheme 2) in the presence of EDCI, HOBT and DIPEA in  $\text{CH}_2\text{Cl}_2$  afforded the dipeptide **27** (74%). Ester **27** on treatment with  $\text{CF}_3\text{COOH}$  in  $\text{CH}_2\text{Cl}_2$  gave the salt **28**, while on base hydrolysis with LiOH it afforded the acid **29**. Coupling (EDCI, HOBT and DIPEA) of acid **29** with salt **30** in  $\text{CH}_2\text{Cl}_2$  furnished the tripeptide **5** in 59% yield. Reaction of acid **5** with  $\text{CF}_3\text{COOH}$  in  $\text{CH}_2\text{Cl}_2$  gave the salt **31**, which on coupling with acid **29** in  $\text{CH}_2\text{Cl}_2$  afforded the pentapeptide **7** in 50% yield. Acid **29** on further coupling with the salt **28** afforded tetrapeptide **6** in 38% yield. Subsequently, peptide **6** on reaction with LiOH gave acid **32**,

Scheme 1. Synthesis of (*R*)- $\beta$ -Caa<sub>(*r*)</sub> **3**<sup>a</sup>

<sup>a</sup>Reagents and conditions: (a) (COCl)<sub>2</sub>, DMSO, Et<sub>3</sub>N, CH<sub>2</sub>Cl<sub>2</sub>, -78 °C, 3 h; (b) NaBH<sub>4</sub>, EtOH/H<sub>2</sub>O (19:1), 0 °C, 1 h; (c) KOH, 1,4-dioxane, reflux; then CH<sub>3</sub>I, 0 °C to rt, 12 h; (d) 60% aq. AcOH, 12 h; (e) NaIO<sub>4</sub>, CH<sub>2</sub>Cl<sub>2</sub>, 0 °C, 6 h; (f) Ph<sub>3</sub>P=CHCO<sub>2</sub>Me, CH<sub>2</sub>Cl<sub>2</sub>, 0 °C to rt, 4 h; (g) BnNH<sub>2</sub>, rt, 12 h; (h) 10% Pd/C, H<sub>2</sub>/MeOH, rt, 12 h; (i) (Boc)<sub>2</sub>O, Et<sub>3</sub>N, CH<sub>2</sub>Cl<sub>2</sub>, 0 °C to rt, 2 h; (j) CF<sub>3</sub>CO<sub>2</sub>H, dry CH<sub>2</sub>Cl<sub>2</sub>, 2 h.

Scheme 2. Synthesis of Mosher Amides of (*R*)- $\beta$ -Caa<sub>(*r*)</sub> **3** and **20**<sup>a</sup>

<sup>a</sup>Reagents and conditions: (a) (*R*)-Ph(OCH<sub>3</sub>)CHCO<sub>2</sub>H, HOBt, EDCl, DIPEA, CH<sub>2</sub>Cl<sub>2</sub>, 0 °C to rt, 8 h; (b) (*S*)-Ph(OCH<sub>3</sub>)CHCO<sub>2</sub>H, HOBt, EDCl, DIPEA, CH<sub>2</sub>Cl<sub>2</sub>, 0 °C to rt, 8 h.

which on coupling with salt **28** in the presence of EDCl, HOBt and DIPEA in CH<sub>2</sub>Cl<sub>2</sub> afforded the hexapeptide **8** in 32% yield. Similarly, acid **32** on coupling (EDCl, HOBt and DIPEA) with salt **31** in CH<sub>2</sub>Cl<sub>2</sub> furnished the heptapeptide **9** (34%, Scheme 3).

## CONFORMATIONAL ANALYSIS

NMR studies<sup>24</sup> on the oligomers **5**–**9** were undertaken in 1–5 mM solution in CDCl<sub>3</sub>, while **8** and **9** were also investigated in CD<sub>3</sub>CN and CD<sub>3</sub>OH. In addition to a major isomer, all of the peptides (in CDCl<sub>3</sub>) showed ubiquitous presence of a minor

isomer, as deduced from the exchange peaks in the ROESY spectra. However, the studies could be carried out only on the major isomer, since the population of the minor isomer was too small to be detected in the one-dimensional <sup>1</sup>H NMR spectra.

The smaller oligomers (**5** and **6**) did not show any well-defined regular structure, though the NMR data, such as the chemical shifts ( $\delta > 7$  ppm) of the amide protons of  $\beta$ -residues and nominally small change in their values ( $\Delta\delta$ ) during solvent titration studies,<sup>24,25</sup> besides few medium range NOE correlations<sup>25</sup> inferred the possibility for a nascent structure.

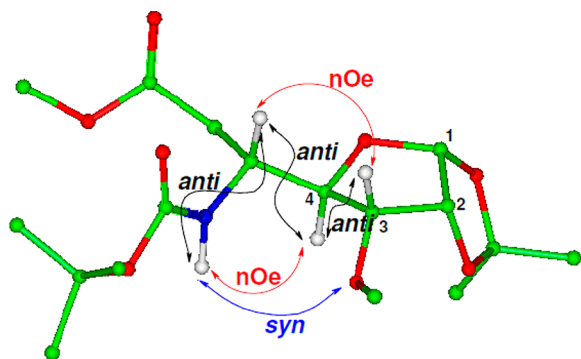


Figure 4. Structure of (*R*)- $\beta$ -Caa(*r*) **3** depicting the proximity of NH and OMe for a possible electrostatic interaction.

**Structural Studies of Peptides 7–9.** Significant information on the H-bonding and folding propensities was realized from the studies on peptides 7–9. For the pentapeptide **7**, backbone resonances were well resolved. Two of the amide protons, NH(2) and NH(4), showed chemical shifts ( $\delta$ NH) > 7 ppm, whereas, in the solvent titration studies<sup>24</sup> (Figure 5) NH(4) alone displayed a small change in the chemical shift ( $\Delta\delta$ ), implying its involvement in H-bonding. Large values of  $^3J_{\text{NH-C}\beta\text{H}} = 8.5$  and 9.0 Hz for the  $\beta$ -residues indicated *anti*-periplanar arrangement of these protons with  $\phi_\beta$  (CO–N–C $\beta$ –C $\alpha$ )  $\approx -120^\circ$ .

In the case of the  $\alpha$ -residues, values of  $^3J_{\text{NH-C}\alpha\text{H}} \approx 6.0$ , 6.5, and 6.9 Hz indicated that there is averaging over several conformations, possibly with preponderance of  $\phi_\alpha$  (CO–N–C $\alpha$ –CO) as  $\sim -60^\circ$  or  $180^\circ$ , specially for the first residue with  $^3J_{\text{NH-C}\alpha\text{H}} = 6.0$  Hz. One large (8.1 Hz) and another small (<3.9 Hz) value for  $^3J_{\text{C}\beta\text{H-C}\alpha\text{H}}$  indicate  $\theta$  (N–C $\beta$ –C $\alpha$ –CO) to be around  $60^\circ$  or  $180^\circ$  (Figure 6).

The C $\alpha$ H resonances of  $\beta$ -residue were stereospecifically assigned from the data on the couplings with C $\beta$ H proton and NOEs with NH protons. Stronger NH/C $\alpha$ H NOE correlations, involving C $\alpha$ H with large  $^3J_{\text{C}\alpha\text{H-C}\beta\text{H}}$  value ( $\sim 8$  Hz) and relatively weak NH/C $\alpha$ H NOE correlations, involving C $\alpha$ H with small  $^3J_{\text{C}\alpha\text{H-C}\beta\text{H}}$  value (<4 Hz), permitted us to confirm  $\theta$

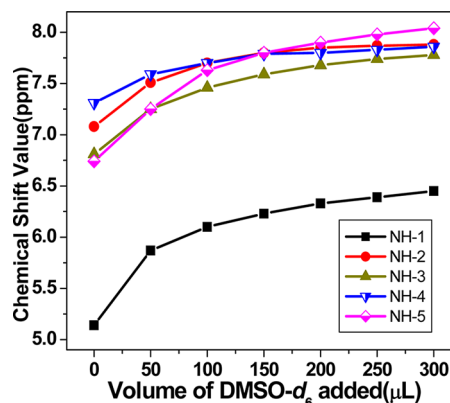


Figure 5. Variation in the NH chemical shifts on addition of DMSO- $d_6$  solvent in 600  $\mu\text{L}$  solution of **7** in  $\text{CDCl}_3$  (600 MHz).

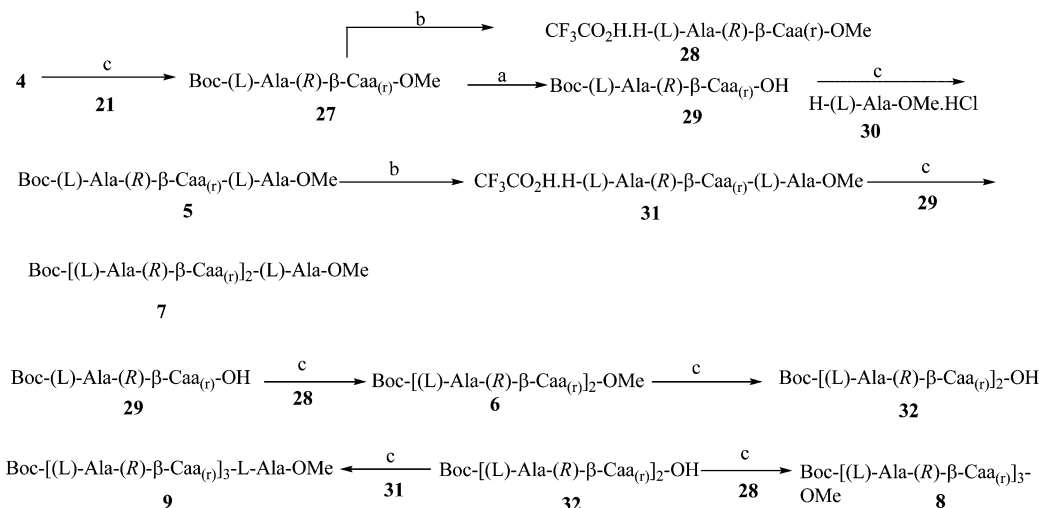
$\approx 60^\circ$  and assign the C $\alpha$ H with large  $^3J_{\text{C}\alpha\text{H-C}\beta\text{H}}$  value as C $\alpha$ H(<sub>pro-R</sub>). Though for the second residue  $^3J_{\text{C}\beta\text{H-C}\alpha\text{H}} = 7.1$  Hz suggests averaging over several conformations about  $\chi_1$ (H–C $\beta$ –C $\alpha$ –H),  $^3J_{\text{C}\beta\text{H-C}\alpha\text{H}} \approx 8.5$  Hz for the fourth residue, indicates predominance of  $\chi_1 \approx 180^\circ$ .

In the ROESY spectrum (Figure 7), medium range NOEs like C $\alpha$ H(1)/NH(4), C $\alpha$ H(1)/C $\alpha$ H(<sub>pro-R</sub>)(4) C $\alpha$ H(1)/C $\alpha$ H(<sub>pro-S</sub>)(4) along with several NH–NH connectivities [NH(1)/NH(2), NH(3)/NH(4), and NH(4)/NH(5)] imply the presence of a secondary structure.

The above inferences on the molecular conformation as well as observation of several NOE correlations between residues *i* and *i*+3 (*i*+3 NOEs) are suggestive of the possible predominance of 11- and 14/15-helix in these oligomers. It was however not possible to discriminate and conclusively comment on the nature of the hydrogen bonding pattern (11- or 14/15-membered) at this stage.

Gellman et al.<sup>5a,8c</sup> have presented the characteristic features for the 11- and 14/15-helices based on the unique NOEs observed in each case, like: C $\alpha$ H(*i*)(A)/NH(*i*+2)(A) for 11-helix and C $\alpha$ H(*i*)(A)/C $\alpha$ H(*i*+3)(B), C $\alpha$ H(*i*)(A)/NH(*i*+4)(A) and C $\beta$ H(*i*)(B)/NH(*i*+4)(B) for 14/15-helix, where A and B are  $\alpha$ - and  $\beta$ -residues respectively. As shown in the Table 1,

### Scheme 3. Synthesis of Peptides 5–9<sup>a</sup>



<sup>a</sup>Reagents and conditions: (a) LiOH, THF/MeOH/H<sub>2</sub>O (3:1:1), 0 °C-rt, 1 h; (b) CF<sub>3</sub>CO<sub>2</sub>H, dry CH<sub>2</sub>Cl<sub>2</sub>, 2 h; (c) HOBT (1.2 equiv), EDCI (1.2 equiv), DIPEA (2 equiv), dry CH<sub>2</sub>Cl<sub>2</sub>, 0 °C-rt, 8 h.

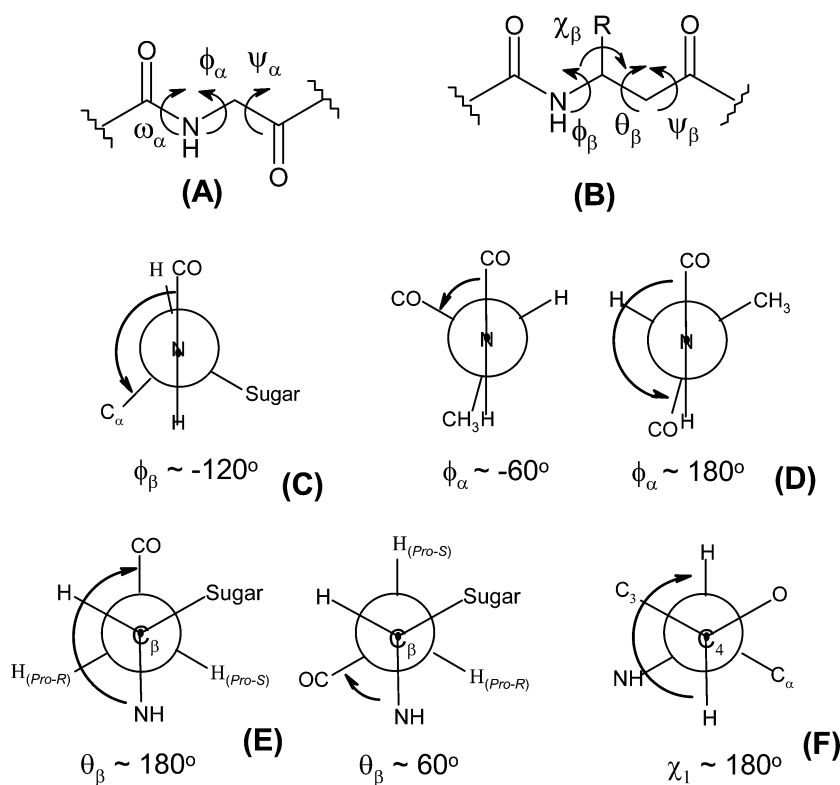


**Figure 6.** Dihedral angles in (A)  $\alpha$ -amino acids and (B)  $\beta$ -amino acids. Probable values of dihedral angles (C) CO–N–C $_{\beta}$ –C $_{\alpha}$  ( $\phi_{\beta}$ ) for a large  $^3J_{\text{NH-C}\beta\text{H}}$  of (R)- $\beta$ -Caa(<sub>r</sub>), (D) CO–N–C $_{\alpha}$ –CO ( $\phi_{\alpha}$ ) for a small  $^3J_{\text{NH-C}\alpha\text{H}}$  of L-Ala, (E) N–C $_{\beta}$ –C $_{\alpha}$ –CO ( $\theta_{\beta}$ ) for a small and a large  $^3J_{\text{C}\alpha\text{H-C}\beta\text{H}}$  of (R)- $\beta$ -Caa and (F) for H–C $_{\beta}$ –C $_{\alpha}$ –H ( $\chi_1$ ) large  $^3J_{\text{C}\beta\text{H-C}\alpha\text{H}}$  for (R)- $\beta$ -Caa(<sub>r</sub>).

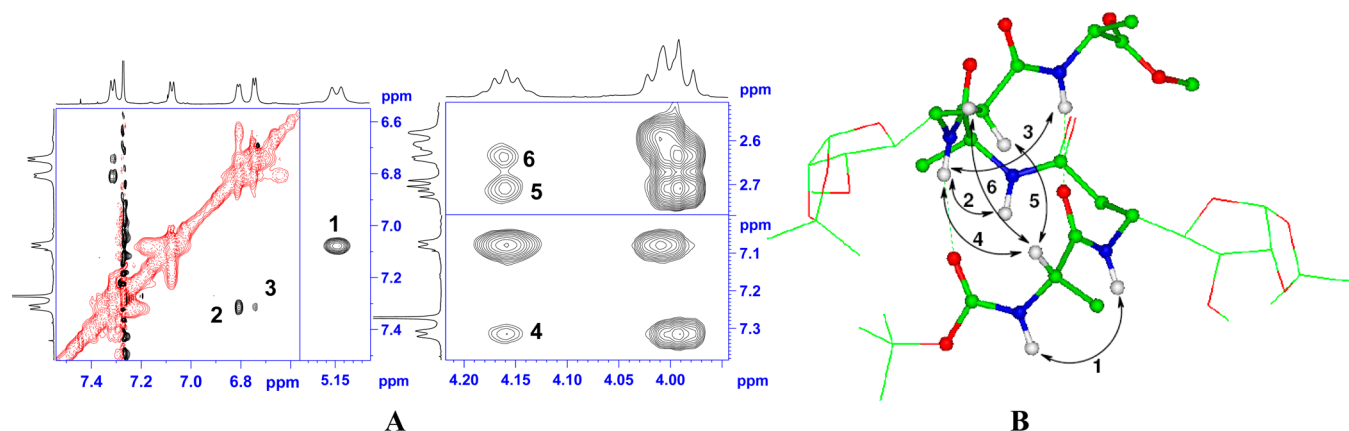


**Figure 7.** (A) ROESY spectrum of **7** in CDCl<sub>3</sub> (600 MHz, 298 K) [the NOEs NH(1)/NH(2), NH(3)/NH(4), NH(4)/NH(5), C $_{\alpha}$ H(1)/NH(4), C $_{\alpha}$ H(1)/C $_{\alpha}$ H<sub>(pro-R)</sub>(4) and C $_{\alpha}$ H(1)/C $_{\alpha}$ H<sub>(pro-S)</sub>(4) are marked as 1–6, respectively]. (B) One minimum energy structure with the same NOE correlations.

unlike in Gellman's prescription for these helices, in the present study, the  $\beta$ -residues have additional C $_{\alpha}$ H<sub>(pro-S)</sub> protons and the associated NOE correlations (marked “\*”) for characterizing these helices. The distances presented in the Table 1 were arrived at from the theoretical studies on geometrical model by Hoffman et al.<sup>16a</sup>

A careful analysis of the observed NOE correlations for **7** revealed the absence of the two possible diagnostic *i*, *i*+2 NOEs [C $_{\alpha}$ H(1)(A)/NH(3)(A), C $_{\alpha}$ H(3)(A)/NH(5)(A)], besides C $_{\alpha}$ H<sub>(pro-S)</sub>(2)(B)/NH(5)(A) attributed exclusively to 11-helix. On the other hand, though C $_{\alpha}$ H(1)(A)/C $_{\alpha}$ H<sub>(pro-R)</sub>(4)(B), characteristic of 14/15-helix was distinctly observed, the other possible NOE i.e. C $_{\alpha}$ H(1)/NH(5) could not be seen, probably

due to fraying at the termini. Likewise, the presence of an exceptional NOE, C $_{\alpha}$ H(1)(A)/C $_{\alpha}$ H<sub>(pro-S)</sub>(4)(B), which could be observed only for  $\alpha/\beta$ -peptides derived from the  $\beta^3$ -residues (Table 1) seems to suggest that in **7**, 14/15-helix might predominate. The results of the present design of  $\alpha/\beta$ -peptides are striking, since it adopted a totally different strategy to obtain the helical folds. Unlike in the earlier studies,<sup>7–9</sup> constraints in the present design are introduced in the  $\beta$ -amino acid residue through additional interactions between the side chain and backbone.

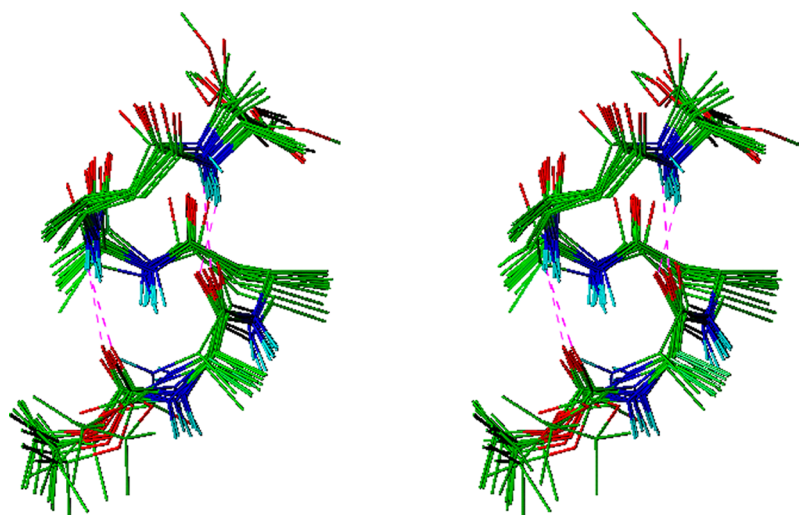
MD calculations for peptide **7** (Figure 8) were performed using the distance constraints, which were applied as flat-bottom potential using a force constant 15 kcal.mol<sup>-1</sup> Å<sup>-2</sup>.

**Table 1.** Characteristic NOEs for 11- and 14/15-Helix Types<sup>a</sup>

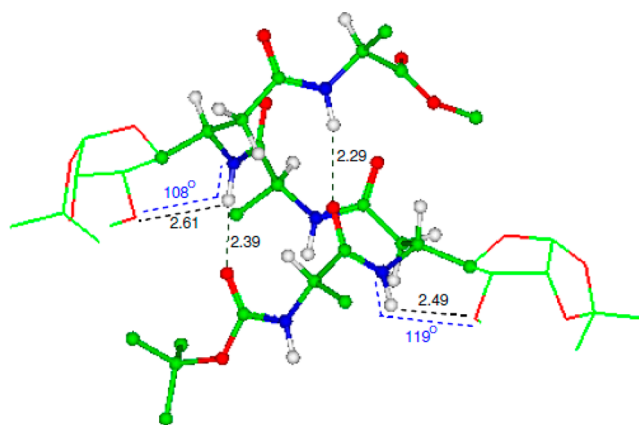
	NOE type	11-helix	14/15-helix
1	C <sub>β</sub> H( <i>i</i> )(B)/NH( <i>i</i> +2)(B)	Yes (3.5 Å)	Yes (4.5 Å)
2	C <sub>β</sub> H( <i>i</i> )(B)/C <sub>α</sub> H <sub>(pro-R)</sub> ( <i>i</i> +2)(B)	Yes (3.8 Å)	Yes (4.6 Å)
3	C <sub>α</sub> H <sub>(pro-R)</sub> ( <i>i</i> )(B)/NH( <i>i</i> +2)(B)	Yes (4.4 Å)	Yes (4.1 Å)
4	C <sub>α</sub> H( <i>i</i> )(A)/NH( <i>i</i> +2)(A) <sup>b</sup>	Yes (3.7 Å)	No (5.7 Å)
5	C <sub>β</sub> H( <i>i</i> )(B)/NH( <i>i</i> +3)(A)	Yes (4.1 Å)	Yes (3.5 Å)
6	C <sub>α</sub> H( <i>i</i> )(A)/NH( <i>i</i> +3)(B)	Yes (3.4 Å)	Yes (3.9 Å)
7	C <sub>α</sub> H( <i>i</i> )(A)/C <sub>α</sub> H <sub>(pro-R)</sub> ( <i>i</i> +3)(B) <sup>c</sup>	No (5.5 Å)	Yes (2.6 Å)
8*	C <sub>α</sub> H( <i>i</i> )(A)/C <sub>α</sub> H <sub>(pro-S)</sub> ( <i>i</i> +3)(B) <sup>c</sup>	No (6.4 Å)	Yes (3.9 Å)
9*	C <sub>α</sub> H <sub>(pro-S)</sub> ( <i>i</i> )(B)/NH( <i>i</i> +3)(A) <sup>b</sup>	Yes (4.4 Å)	No (5.4 Å)
10	C <sub>α</sub> H( <i>i</i> )(A)/NH( <i>i</i> +4)(A) <sup>c</sup>	No (6.5 Å)	Yes (3.6 Å)
11	C <sub>β</sub> H( <i>i</i> )(B)/NH( <i>i</i> +4)(B) <sup>c</sup>	No (6.6 Å)	Yes (3.8 Å)

<sup>a</sup>C<sub>α</sub>H<sub>(pro-S)</sub> proton; A/B represent  $\alpha$ -/ $\beta$ -residues; yes/no implies the presence/absence of NOE for a specific helix, when interproton distances (paranthesis) are less or greater than 5 Å. NOEs unique to: <sup>b</sup>11-helix. <sup>c</sup>14/15-helix. \* NOEs unique to C<sub>α</sub>H<sub>(pro-S)</sub>

These constraints were obtained from two-spin approximation and the volume integrals of NOE peaks from the ROESY spectrum. Two sets of MD calculations, starting with initial structures having 14/15-helical folds ( $\phi_\alpha \approx -70^\circ$ ,  $\psi_\alpha \approx -30^\circ$ ,  $\phi_\beta \approx -120^\circ$ ,  $\theta_\beta \approx 80^\circ$ ,  $\psi_\beta \approx -120^\circ$ ) and the 11-helix ( $\phi_\alpha \approx -70^\circ$ ,  $\psi_\alpha \approx -20^\circ$ ,  $\phi_\beta \approx -90^\circ$ ,  $\theta_\beta \approx 80^\circ$ ,  $\psi_\beta \approx -90^\circ$ ), were carried out, which however converged into similar structures.<sup>16a</sup> In view of the above NMR and MD data, further MD calculations were carried out starting with the structural parameters of 14/15-helix only. The superposition of 15 minimum energy structures resulted in backbone and heavy atom rmsd values of 1.05 Å and 1.17 Å respectively (Figure 8) with rather large distance violations (<0.73 Å). The first and the last residues display a considerable amount of fraying, reflecting disorderliness in the structures. The average backbone dihedral angles, excluding the terminal residues are:  $\phi_\alpha \approx -78 \pm 4^\circ$ ,  $\psi_\alpha \approx -70 \pm 4^\circ$ ,  $\phi_\beta \approx -96 \pm 3^\circ$ ,  $\theta_\beta \approx 77 \pm 5^\circ$ ,  $\psi_\beta \approx -95 \pm 9^\circ$ . Though for  $\psi_\alpha$  a value of  $\sim -70^\circ$  appears to considerably differ from that reported by Hofmann et al.,<sup>16a</sup> the H-bonding involving the amide protons of the fourth and fifth residues with the backbone carbonyl groups (NH(4)...O=C-

**Figure 8.** Stereoview of 15 superimposed minimum energy structures for peptide 7 (the sugar moieties were replaced by methyl groups after the calculations for clarity).

Boc and NH(5)... O=C(1)) sustain a 14/15-helix. The significant deviations observed in the MD structures possibly arise partly due to the fact that a pentapeptide has too few residues to exclusively support a 14/15-helix and partly due to the disproportionately large contribution to the intraresidue and the sequential NOEs from other disordered structures. These structures also showed that, NH(2) and NH(4) come close to the sugar oxygen of OMe at C-3 position, supporting the possibility of a weak intraresidue electrostatic interaction (N-H...O(Me) distance of  $\sim 2.5$ – $3.0$  Å and  $\angle$  N-H...O(Me)  $\approx 105$ – $120^\circ$ ) as envisaged by us while designing the monomer. One of the minimum energy structures obtained during the MD studies is shown in the Figure 9.

**Figure 9.** One of the minimum energy structures of 7 showing NH...O distances (Å) (black) and NH...OMe angles (blue).

NMR data,  $\delta$ NH(2) = 7.07 ppm and  $\Delta\delta$ NH(2) = 0.80 ppm, also support the above findings with the possibility of significant population of conformers displaying the electrostatic interaction, as was noticed in smaller oligomers 5 and 6.<sup>24,25</sup> We conclude that the proximity of OMe and amide protons of the second and the fourth residue, might be providing a small additional electrostatic interaction to nucleate the helical structure as was reported for the oligomers of  $\beta^{2,2}$ -Caa.<sup>19</sup>

It was not possible from these NMR experiments to directly pronounce the details of H-bonding and hence no restraints for hydrogen bonds were introduced in the structure determination process. However, by simple inspection of the structural bundles obtained subsequently, the presence of an electrostatic interaction between amide protons to the oxygen of the methoxy side chain of sugar groups was observed. The intrasidue electrostatic interaction<sup>19</sup> might be an important additional contribution, which facilitates the formation of the secondary structure in these  $\alpha/\beta$ -peptides containing  $\beta$ -amino acids with carbohydrate side chains (Figure 9).

For hexapeptide **8** in  $\text{CDCl}_3$  solution, backbone resonances were well resolved.<sup>24</sup> Low field chemical shifts of the amide protons ( $\delta_{\text{NH}} > 7$  ppm), except NH(1) and NH(2), suggested their participation in H-bonding. This was further confirmed by solvent titration studies.<sup>25</sup> Coupling constants were similar to that of **7**, suggesting analogous structure. However, because of overlap of  $\text{C}_\alpha\text{H}(1)$ ,  $\text{C}_\alpha\text{H}(3)$  and  $\text{C}_\beta\text{H}(4)$  resonances, the two possible  $i, i+2$  NOEs for 11-helix [ $\text{C}_\alpha\text{H}(1)(\text{A})/\text{NH}(3)(\text{A})$ ,  $\text{C}_\alpha\text{H}(3)(\text{A})/\text{NH}(5)(\text{A})$ ] could not be ascertained, while  $\text{C}_\alpha\text{H}_{(\text{pro-S})}(2)(\text{B})/\text{NH}(5)(\text{A})$ , the other characteristic NOE of 11-helix was absent. Similar reasons hindered in distinctly defining the NOE characteristics of 14/15-helix such as  $\text{C}_\alpha\text{H}(1)(\text{A})/\text{C}_\alpha\text{H}_{\text{pro-R/S}}(4)(\text{B})$ ,  $\text{C}_\alpha\text{H}(3)(\text{A})/\text{C}_\alpha\text{H}_{\text{pro-R/S}}(6)(\text{B})$  and  $\text{C}_\alpha\text{H}(1)(\text{A})/\text{NH}(5)(\text{A})$ . In addition, another characteristic NOE  $\text{C}_\beta\text{H}(2)(\text{B})/\text{NH}(6)(\text{B})$  of 14/15-helix, was ambiguous because of the overlap of  $\text{C}_\beta\text{H}(2)$  and  $\text{C}_\beta\text{H}(6)$ . Thus, the discrimination of the two helical structures was not possible in **8**.

To deduce additional structural information on **8**, it was also studied in  $\text{CD}_3\text{CN}$  and  $\text{CD}_3\text{OH}$ .<sup>24</sup> Though, well resolved resonances were observed in  $\text{CD}_3\text{CN}$ , the absence of NOEs specific to 11- or 14/15-helices (Table 1), prevented us from defining the helical pattern.<sup>24</sup> On the other hand, the NMR in  $\text{CD}_3\text{OH}$  displayed severe overlap, with a very few resolved NOEs. However, presence of weak signatures for helical structures were confirmed by  $^1\text{H}$ - $^2\text{H}$  exchange studies in  $\text{CD}_3\text{OD}$ .<sup>24</sup>

The  $^1\text{H}$  NMR spectrum of peptide **9** in  $\text{CDCl}_3$  showed broad resonances.<sup>24</sup> On standing at room temperature, within 8 h (and even faster at low temperatures) the solution aggregate to form a gel. Therefore the structure was investigated in methanol- $d_3$  and acetonitrile- $d_3$  solutions.

The NMR spectrum of **9** in methanol- $d_3$  (at 279 K) showed the presence of two isomers as indicated by the presence of exchange peaks in the ROESY spectrum.<sup>24</sup> However, the population of the minor isomer was very small (probably <1%) and could not be studied. For the major isomer, the couplings were very similar to those observed for other peptides in  $\text{CDCl}_3$ .<sup>24</sup> The dihedral angle  $\phi_\beta$  for all the  $\beta$ -Caa residues was found to be restricted to  $\sim -120^\circ$  based on the  $^3J_{\text{NH-C}\beta\text{H}}$  values of  $\sim 9$  Hz. On the other hand, for  $\alpha$ -residues,  $^3J_{\text{NH-C}\alpha\text{H}} < 6.2$  Hz, suggests  $\phi_\alpha \approx -60^\circ$ . Though  $^3J_{\text{C}\beta\text{H-C}\alpha\text{H}}$  could not be derived for most of the  $\beta$ -residues, the values obtained were consistent with the proposed structure discussed for **7**.

In the exchange studies (Figure 10) for **9** in methanol- $d_4$ , most of the amide protons did not exchange fully even after 5 h, indicating a weak secondary structure. The NH(1), NH(3) and NH(7) were the first to exchange, disappearing completely after  $\sim 3$  h. Though NH(2), NH(4), NH(5), and NH(6) could be seen even after 5 h, none of the amide proton resonances was observed after 19 h, indicating probability for the presence of a well-defined structure, but as a small population. It appears

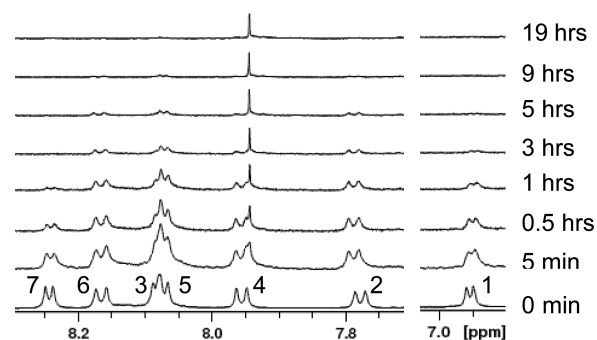


**Figure 10.** NMR spectra of the amide region of **9** as a function of time after dissolving in  $\text{CD}_3\text{OD}$  (600 MHz; amide protons assignments are marked as 1–7).

yet again that NH(2) behaves like most of the amide protons at the C-terminal, confirming its involvement in the anticipated electrostatic interaction.

In the ROESY spectrum of **9** due to severe overlap, only three unambiguous NOE correlations defining 11- and 14/15-helix (Table 1) could be deduced. Thus, to ascertain more structural information on **9**, studies were undertaken in  $\text{CD}_3\text{CN}$  solution. Peptide **9** showed very poor solubility in acetonitrile and the resonances were broadened. However, the studies of the saturated solution (concentration <1.5 mM) could still be carried out as the spectral dispersion was good, indicating presence of a well-defined structure. The presence of a minor isomer, like that in methanol (population <1%), was deduced from the exchange peaks of the ROESY spectrum. In the  $^1\text{H}$  NMR spectrum (283 K), NH(5), NH(6) and NH(7) have  $\delta > 7.3$  ppm, suggesting their involvement in hydrogen bonding.<sup>24</sup> However, in solvent titration studies<sup>25</sup> (15% (v/v) of  $\text{DMSO-}d_6$  was sequentially added to the solution of the peptide in  $\text{CD}_3\text{CN}$ ) only NH(5) and NH(6) were found to be H-bonded as they showed small changes in their chemical shifts ( $\Delta\delta_{\text{NH}} < 0.2$  ppm). Furthermore,  $\Delta\delta_{\text{NH}}(4) = 0.40$  ppm and  $\Delta\delta_{\text{NH}}(7) = 0.48$  ppm, may imply the presence of significant populations of **9**, wherein, NH(4) and NH(7) participate in H-bonding.

$^3J_{\text{NH-}\beta\text{H}} > 9.2$  Hz for the  $\beta$ -residue indicated an *anti*-periplanar arrangement of these protons with  $\phi \approx -120^\circ$ . On the other hand,  $^3J_{\text{NH-C}\alpha\text{H}} < 5.5$  Hz correspond to the value of  $\phi \approx -60^\circ$  or  $180^\circ$  for the  $\alpha$ -residues. For NH(7), a larger  $^3J_{\text{NH-C}\alpha\text{H}}$  (6.4 Hz) might be a reflection of fraying at the terminus. The  $\text{C}_\alpha\text{H}_{(\text{pro-R})}$  and  $\text{C}_\alpha\text{H}_{(\text{pro-S})}$  resonances were assigned using only the NOEs,  $\text{NH}(i)/\text{C}_\alpha\text{H}_{(\text{pro-R})}(i)$  and  $\text{C}_\alpha\text{H}_{(\text{pro-R})}(i)/\text{NH}(i+1)$ , since all the  $^3J_{\text{C}\beta\text{H-C}\alpha\text{H}}$  could not be obtained (except for the second residue).

The  $^3J_{\text{C}4\text{H-C}\beta\text{H}}$  values of <8 Hz in  $\text{CD}_3\text{CN}$  (compared to >8 Hz in  $\text{CD}_3\text{OH}$ ), showed the possible presence of larger population of other rotamers about  $\text{C}_\beta\text{-C}_4$  bonds. This was further supported by the NOEs which differ from those observed in  $\text{CDCl}_3/\text{CD}_3\text{OH}$ .

Many of the characteristic  $i \rightarrow i+3$  and  $i \rightarrow i+4$  NOEs like:  $\text{C}_\alpha\text{H}(1)(\text{A})/\text{NH}(4)(\text{B})$ ,  $\text{C}_\beta\text{H}(2)(\text{B})/\text{NH}(5)(\text{A})$ ,  $\text{C}_\beta\text{H}(2)(\text{B})/\text{NH}(6)(\text{B})$ ,  $\text{C}_\alpha\text{H}(3)(\text{A})/\text{NH}(6)(\text{B})$  and  $\text{C}_\alpha\text{H}(3)(\text{A})/\text{C}_\alpha\text{H}(6)(\text{B})$  were identified without ambiguity (Figure 11). The helical signatures attributed to the presence of  $\text{NH}(i)/\text{NH}(i+1)$  NOE correlations were poorly displayed, while the NOEs  $\text{NH}(1)/\text{NH}(2)$  and  $\text{NH}(3)/\text{NH}(4)$  were only observed. It was reasoned that the NOE correlations were clouded due to the presence of significant exchange peaks between major and



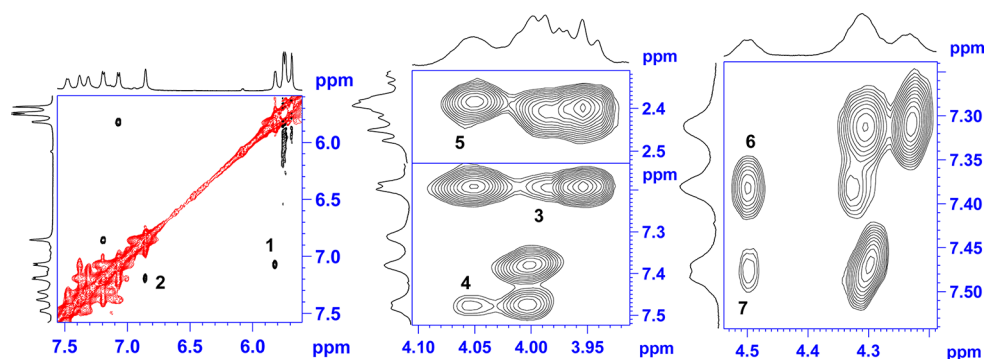


**Figure 11.** ROESY spectrum of **9** in  $\text{CD}_3\text{CN}$  (600 MHz, 283 K) (the NOEs  $\text{NH}(1)/\text{NH}(2)$ ,  $\text{NH}(3)/\text{NH}(4)$ ,  $\text{C}_\alpha\text{H}(1)/\text{NH}(4)$ ,  $\text{C}_\alpha\text{H}(3)/\text{NH}(6)$ ,  $\text{C}_\alpha\text{H}(3)(\text{A})/\text{C}_\alpha\text{H}_{\text{pro-R/S}}(6)(\text{B})$ ,  $\text{C}_\beta\text{H}(2)/\text{NH}(5)$  and  $\text{C}_\beta\text{H}(2)/\text{NH}(6)$  are marked as 1–7 respectively).

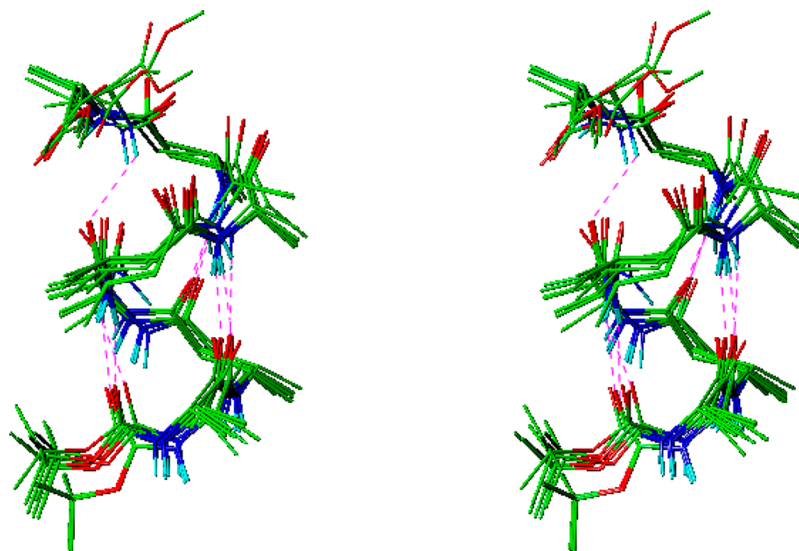


**Figure 12.** Side-view of superimposed 15 minimum energy structures of **9** (sugars are replaced with methyls for clarity).

minor isomers. For the heptapeptide **9**, out of the three possible characteristic NOEs for 11-helix, two [ $\text{C}_\alpha\text{H}(1)(\text{A})/\text{NH}(3)(\text{A})$ ,  $\text{C}_\alpha\text{H}(5)(\text{A})/\text{NH}(7)(\text{A})$ ] seem to be absent, while the other NOEs such as  $\text{C}_\alpha\text{H}(3)(\text{A})/\text{NH}(5)(\text{A})$ ,  $\text{C}_\alpha\text{H}_{\text{pro-S}}(2)(\text{B})/\text{NH}(5)(\text{A})$  and  $\text{C}_\alpha\text{H}_{\text{pro-S}}(4)(\text{B})/\text{NH}(7)(\text{A})$  could not be ascertained because of overlap of  $\text{C}_\alpha\text{H}(3)$  with  $\text{C}_\alpha\text{H}(5)$  and  $\text{C}_\alpha\text{H}_{\text{pro-S}}(2)$  with  $\text{C}_\alpha\text{H}_{\text{pro-S}}(4)$  protons. However, the characteristic NOE  $\text{C}_\beta\text{H}(2)(\text{B})/\text{NH}(6)(\text{B})$  for 14/15-helix could be specifically assigned. Though another NOE unique to 14/15-helix, between  $\text{C}_\alpha\text{H}(3)(\text{A})$  and  $\text{C}_\alpha\text{H}(6)(\text{B})$  was also observed, due to spectral overlap prochiral assignment for  $\text{C}_\alpha\text{H}(6)(\text{B})$  could not be made. The remaining NOEs like  $\text{C}_\alpha\text{H}(1)(\text{A})/\text{C}_\alpha\text{H}_{\text{pro-R}}(4)(\text{B})$  and  $\text{C}_\alpha\text{H}(1)(\text{A})/\text{NH}(5)(\text{A})$  could not be assigned because of overlap of  $\text{C}_\alpha\text{H}(1)$ ,  $\text{C}_\alpha\text{H}(5)$  and  $\text{C}_4\text{H}(4)$ , while  $i/i+4$  NOE  $\text{C}_\alpha\text{H}(3)(\text{A})/\text{NH}(7)(\text{A})$  could not be seen due to probable fraying at the terminal residue.

The MD calculations for **9** were performed following the protocol adopted for **7**, however, to simulate the  $\text{CD}_3\text{CN}$  environment, distance dependent dielectric constants ( $\epsilon$ ) value of 37.5 was used. Through superposition of 15 minimum energy structures of **9** that emerged from MD calculations (Figure 12), the backbone and heavy atom rmsd values were found to be 0.72 and 1.12 Å respectively, with none of the distance violations  $>0.30$  Å.

In the above superimposed structures of **9**, the backbone heavy atoms display a much smaller rmsd value compared to that for **7**, suggesting a better definition of the 14/15-helix. The average backbone dihedral angles, excluding the terminal residues were found to be  $\phi_\alpha \approx -77 \pm 11^\circ$ ,  $\psi_\alpha \approx -45 \pm 14^\circ$ ,  $\phi_\beta \approx -101 \pm 6^\circ$ ,  $\theta_\beta \approx 72 \pm 4^\circ$ ,  $\psi_\beta \approx -121 \pm 26^\circ$ .

Unlike in **7**, the backbone dihedral angles for **9** are quite close to the values expected for an ideal 14/15-helix, proposed theoretically by Hofmann et al.<sup>16a</sup> In addition, for **7** and **9**, the average  $\text{NH}\cdots\text{O}(\text{Me})$  distances are  $2.60 \pm 0.06$  Å and  $2.94 \pm 0.10$  Å respectively. From the above findings it is clear that the higher oligomer generates a more robust helical structure probably due to the presence of increased number of hydrogen bonds.

In peptides **7** and **9**, the couplings,  $^3J_{\text{C}_1\text{H}-\text{C}_2\text{H}} \sim 4$  Hz,  $^3J_{\text{C}_2\text{H}-\text{C}_3\text{H}} \approx 4$  Hz, and  $^3J_{\text{C}_3\text{H}-\text{C}_4\text{H}} \approx 8$  Hz, observed for the carbohydrate side chain of (*R*)- $\beta$ -Caa(*r*) **3**, differ from that of (*R*)- $\beta$ -Caa(*x*) **2**, used in our earlier studies,<sup>12,15</sup> due to the inversion at  $\text{C}_3$  stereocenter in the new monomer. However, the sugar pucker remained the same in both these monomers and corresponds to a  $^3\text{T}_2$  conformation. For **3**, strong NOEs between  $\text{Me}_{(\text{pro-R})}/\text{C}_1\text{H}$  and  $\text{Me}_{(\text{pro-R})}/\text{C}_2\text{H}$  as well as weak  $\text{Me}_{(\text{pro-S})}/\text{C}_4\text{H}$  NOEs further support the envelope conformation of the isopropylidene ring.

CD spectroscopy has been extensively used for elucidating the folding propensities of natural proteins and peptides,<sup>26</sup> yet

it has not been used with the same regularity for  $\beta$ - and  $\alpha/\beta$ -peptides.<sup>27</sup> This is partly due to fact that the database for a variety of  $\beta$ -amino acids is rather small, besides the thinly available high quality structural information for correlation and validation.<sup>9,27,28</sup> The CD spectra of peptides 5–9 (Figure 13),

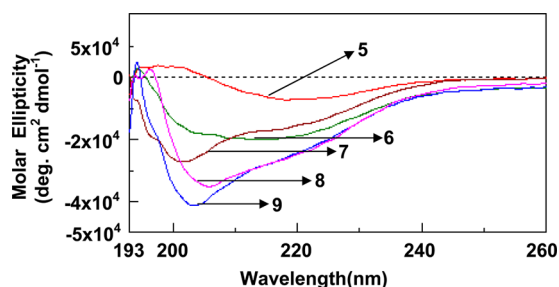


Figure 13. CD spectra of the peptides 5–9 in MeOH.

scanned from 193 to 260 nm as 0.2 mM solutions in methanol, are presented in the Figure 13. For 7 and 9 the CD patterns are almost identical with the minima at 203 and 201 nm (minima around 204 nm is attributed to 14/15-helix<sup>27</sup>) respectively with a shoulder at about 220 nm. The CD spectrum of 8 differs from those of 7 and 9 in having the minima at about 206 nm and having a more pronounced shoulder at around 220 nm. The molar ellipticities of about 27000, 35000, and 41000 for 7, 8 and 9 respectively are quite modest compared to those observed for some other  $\beta$ - and  $\alpha/\beta$ -peptides<sup>2f,3a,12a,15</sup> displaying robust helical structures and suggest that the folds in these peptides are weak in methanol.

## CONCLUSIONS

The present study reports the design and synthesis of a new  $\beta$ -amino acid, (*R*)- $\beta$ -Caa<sub>(r)</sub>, wherein the intraresidue constraints were anticipated to introduce additional electrostatic interactions to facilitate the creation of novel folds. The design of  $\alpha/\beta$ -peptides from (*R*)- $\beta$ -Caa<sub>(r)</sub> and L-Ala, demonstrated the realization of a reasonably robust 14/15-helix from the new  $\beta$ -amino acid. The helical stability in these peptides evidently arises through the additional electrostatic interactions, involving the intraresidue amide proton and C3–OMe of the carbohydrate side chain. Unlike in the earlier reports on 14/15-helix, where constrained cyclic  $\beta$ - or  $\alpha$ -amino acids were utilized in the design of peptides, the present study utilized the new  $\beta$ -amino acid with additional constraints. These results thus provide an opportunity to design new amino acids with a tendency to result in additional interactions. The interaction with a side chain can be used as constraint for the stabilization of helices similar to salt bridges and pi–pi stacking in the alpha helices, thereby expanding the domain of the research.

## EXPERIMENTAL SECTION

NMR spectra (1D and 2D experiments) for peptides 5–9 were obtained at 300, 400, 500, 600 and 700 MHz (<sup>1</sup>H), and at 75, 100, 150 and 175 MHz (<sup>13</sup>C). Chemical shifts are reported in  $\delta$  scale with respect to internal TMS reference. Information on hydrogen bonding in CDCl<sub>3</sub> was obtained from solvent titration studies by sequentially adding up to 300  $\mu$ L of DMSO-*d*<sub>6</sub> in 600  $\mu$ L of CDCl<sub>3</sub> solution of peptides. States-TPPI procedure was used to run various NMR experiments in the phase sensitive mode<sup>29</sup> using standard programs in the library provided by the instrument manufacturer. The ROESY experiments were performed with mixing time of 300 ms using a continuous spin-locking field of about 2.5 kHz. The TOCSY

experiments were performed with the spin locking field of about 10 kHz and a mixing time of 80 ms. The 2D data were processed with Gaussian apodization in both the dimensions. Using two spin approximation and a reference distance of 1.8 Å for the geminal protons at C<sub>w</sub>, the distance constraints were derived from the volume integrals of the cross peaks in the ROESY spectra. Whenever the geminal protons were merged, the sugar proton (C<sub>1</sub>H–C<sub>2</sub>H distance of 2.4 Å) was used as reference.

The CD spectra were obtained in rectangular fused quartz cells of 0.2 cm path length at room temperature with a scan range of 190–260 nm and scanning speed of 50 nm/min, using peptide concentrations of 0.2 mM in MeOH. Binomial method was used for smoothening the spectra. The values are expressed in terms of  $[\theta]$ , the total molar ellipticity (deg cm<sup>2</sup> dmol<sup>-1</sup>).

The Insight-II (97.0)/Discover program was used for construction of molecular model and for structural analysis of different obtained conformations, including molecular modeling calculations and energy minimization. The CVFF force field with default parameters was used throughout the calculations with the aid of a distance dependent dielectric constant with dielectric constant ( $\epsilon$ ) = 4.7 for CDCl<sub>3</sub> and 37.5 for CD<sub>3</sub>CN. The upper and lower bound of the distance constraints have been obtained by enhancing and reducing the derived distance by 10%. The complete set of distance constraints used for peptides 7 and 9 have been tabulated in the Supporting Information, which were used throughout the MD calculations. No constraints for dihedral angle and hydrogen bonding were applied in the MD calculations. For the initiation of the dynamics the molecular model was built based on the angles given for 14/15-helices by Hofmann et al. in their theoretical studies.<sup>16a</sup> Following general protocol was used for minimizing energy. Initial minimizations were done with steepest descent, followed by conjugate gradient methods for a maximum of 5000 iterations each or rms deviation of 0.001 kcal/mol, whichever was earlier. The molecules were initially equilibrated for 1 ps and subsequently subjected to a 2 ns MD run using simulated annealing protocol. Starting from 300 K, they were heated to 1500 K in four steps increasing the temperature (300 K/step) and simulating for 2.5 ps at each step, and then subsequently cooling back to 300 K in 4 steps decreasing the temperature by 300 K and again simulating for 2.5 ps at each cooling step. After this, a structure was saved and the above process was repeated 100 times. The 100 structures generated so were energy minimized with the above protocol and fifteen of the best possible structures were superimposed for display.

The HRMS data were obtained using Q-TOF mass spectrometer. **(3*R*,5*S*,6*R*,6*aR*)-5-((*S*)-2,2-Dimethyl-1,3-dioxolan-4-yl)-2,2-dimethyl-tetrahydrofuro[2,3-*d*][1,3]dioxol-6-ol (12)**. To a stirred solution of 11 (9.0 g, 38 mmol) in aq. ethanol (EtOH: H<sub>2</sub>O 19:1; 100 mL), NaBH<sub>4</sub> (0.73 g, 19.37 mmol) was added at 0 °C and the reaction mixture stirred for 1 h. Solvent was evaporated *in vacuo*, residue treated with sat. NH<sub>4</sub>Cl solution (20 mL) and stirred at room temperature for an additional 10 min. The reaction mixture was extracted with EtOAc (2 × 100 mL) and organic layer separated was washed with water (100 mL), brine (100 mL), dried (Na<sub>2</sub>SO<sub>4</sub>) and evaporated. Residue obtained was purified by column chromatography (60–120 mesh Silica gel, 60% ethyl acetate in pet. ether) to afford 12 (7.0 g, 77%) as a white solid; mp 82 °C;  $[\alpha]_D^{20} = +82.49$  (*c* 1.03, CHCl<sub>3</sub>); IR (KBr): 3413, 2995, 2928, 1634, 1379, 1224, 1164, 1075, 1018 cm<sup>-1</sup>; <sup>1</sup>H NMR (300 MHz, CDCl<sub>3</sub>, 298 K):  $\delta$  5.75 (d, 1H, *J* = 3.7 Hz, C<sub>1</sub>H), 4.56 (t, 1H, *J* = 4.2 Hz, C<sub>2</sub>H), 4.23 (m, 1H, C<sub>5</sub>H), 4.07–3.91 (m, 3H, C<sub>4</sub>H, 2 × C<sub>6</sub>H), 3.74 (dd, 1H, *J* = 8.0, 4.3 Hz, C<sub>3</sub>H), 2.44 (d, 1H, *J* = 8.4 Hz, OH), 1.56 (s, 3H, CH<sub>3</sub>), 1.44 (s, 3H, CH<sub>3</sub>), 1.36 (s, 6H, 2 × CH<sub>3</sub>); <sup>13</sup>C NMR (75 MHz, CDCl<sub>3</sub>, 298 K):  $\delta$  112.8, 109.8, 103.9, 79.7, 79.0, 75.5, 72.5, 65.8, 26.6, 26.5, 26.3, 25.3; HRMS (ESI+): *m/z* calculated for C<sub>12</sub>H<sub>20</sub>O<sub>6</sub> (M<sup>+</sup> + Na) 283.1157, found 283.1171.

**5-[2,2-Dimethyl-(4*R*)-1,3-dioxolan-4-yl]-2,2-dimethyl-(3*aR*,5*R*,6*R*,6*aR*)-perhydrofuro[2,3-*d*][1,3]dioxol-6-yl Methyl Ether (13)**. To a solution of 12 (7.0 g, 26 mmol) in 1,4-dioxane (100 mL), KOH (4.52 g, 80 mmol) was added and heated at reflux for 1 h. The reaction mixture was cooled to 0 °C, MeI (3.4 mL, 53 mmol) added and stirred at room temperature for 12 h. Solvent was

evaporated from the reaction mixture, residue diluted with water (100 mL) and extracted with EtOAc (3 × 100 mL). Organic layer was washed with brine (100 mL), dried (Na<sub>2</sub>SO<sub>4</sub>) and evaporated under reduced pressure. The residue was purified by column chromatography (60–120 mesh Silica gel, 10% ethyl acetate in pet. ether) to give **13** (6.0 g, 80%) as a yellow oil; [ $\alpha$ ]<sub>D</sub><sup>20</sup> = +179.81 (*c* 0.63, CHCl<sub>3</sub>); IR (KBr): 3421, 2935, 2928, 1717, 1379, 1218, 1118, 1080, 1024 cm<sup>-1</sup>; <sup>1</sup>H NMR (500 MHz, CDCl<sub>3</sub>, 298 K):  $\delta$  5.78 (d, 1H, *J* = 3.7 Hz, C<sub>1</sub>H), 4.71 (t, 1H, *J* = 3.9 Hz, C<sub>2</sub>H), 4.39 (dt, 1H, *J* = 3.1, 7.3 Hz, C<sub>5</sub>H), 4.06 (dd, 1H, *J* = 9.1, 3.1 Hz, C<sub>4</sub>H), 4.02 (m, 2H, C<sub>6</sub>H), 3.77 (dd, 1H, *J* = 8.9, 4.1 Hz, C<sub>3</sub>H), 3.51 (s, 3H, OMe), 1.59 (s, 3H, Me), 1.46 (s, 3H, Me), 1.39 (m, 3H, Me), 1.37 (m, 3H, Me); <sup>13</sup>C NMR (75 MHz, CDCl<sub>3</sub>, 298 K):  $\delta$  112.8, 109.6, 103.5, 80.2, 77.5, 77.2, 74.6, 64.9, 58.1, 26.6, 26.3, 26.0, 25.1; HRMS (ESI+): *m/z* calculated for C<sub>13</sub>H<sub>22</sub>O<sub>6</sub> [M<sup>+</sup> + Na] 297.1314, found 297.1305.

**1-[6-Methoxy-2,2-dimethyl-(3aR,5R,6S,6aR)-perhydrofuro[2,3-d][1,3]dioxol-5-yl]-(1R)-ethane-1,2-diol (14)**. A mixture of **13** (3.6 g, 13.1 mmol) in 60% aq. AcOH (25 mL) was stirred at room temperature for 12 h. Reaction mixture was neutralized with anhydrous NaHCO<sub>3</sub> (15 g) and extracted with EtOAc (3 × 50 mL). The combined organic layers were dried (Na<sub>2</sub>SO<sub>4</sub>), evaporated and residue purified by column chromatography (60–120 mesh Silica gel, 50% ethyl acetate in pet. ether) to afford **14** (2.6 g, 85%) as a pale-yellow solid; mp 106 °C; [ $\alpha$ ]<sub>D</sub><sup>20</sup> = +264.93 (*c* 0.5, CHCl<sub>3</sub>); IR (KBr): 3525, 3484, 3376, 2992, 2947, 1217, 1164, 1024, cm<sup>-1</sup>; <sup>1</sup>H NMR (300 MHz, CDCl<sub>3</sub>, 298 K):  $\delta$  5.74 (d, 1H, *J* = 3.7 Hz, C<sub>1</sub>H), 4.65 (t, 1H, *J* = 4.0 Hz, C<sub>2</sub>H), 3.99–3.95 (m, 2H, C<sub>4</sub>H, C<sub>5</sub>H), 3.77–3.64 (m, 3H, C<sub>3</sub>H, 2 × C<sub>6</sub>H), 3.49 (s, 3H, OMe), 2.45 (bs, 1H, OH) 1.56 (s, 3H, Me), 1.50 (bs, 1H, OH), 1.35 (s, 3H, Me); ESIMS *m/z* [M<sup>+</sup> + Na] calculated for C<sub>10</sub>H<sub>18</sub>O<sub>6</sub> 257.1001, found 257.0991.

**Methyl 3-[6-Methoxy-2,2-dimethyl-(3aR,5R,6R,6aR)-perhydrofuro[2,3-d][1,3]dioxol-5-yl]-(E)-2-propenoate (15)**. To a solution of diol **14** (2.7 g, 11.5 mmol) in CH<sub>2</sub>Cl<sub>2</sub> (10 mL), NaIO<sub>4</sub> (3.7 g, 17.3 mmol) was added at 0 °C and stirred at room temperature for 6 h. The reaction mixture was filtered and washed with CH<sub>2</sub>Cl<sub>2</sub> (2 × 20 mL). It was dried (Na<sub>2</sub>SO<sub>4</sub>) and evaporated to give aldehyde **14a** (1.5 g) in quantitative yield as a yellow liquid, which was used as such for the next reaction.

To a solution of the above aldehyde **14a** (1.5 g, 5.49 mmol) in dry CH<sub>2</sub>Cl<sub>2</sub> (5 mL), (methoxycarbonylmethylene) triphenyl phosphorane (2.29 g, 8.24 mmol) dissolved in dry CH<sub>2</sub>Cl<sub>2</sub> (10 mL) was added at 0 °C and stirred at room temperature for 4 h. Solvent was evaporated and residue purified by column chromatography (60–120 mesh Silica gel, 15% ethyl acetate in pet. ether) to afford ester **15** (1.60 g, 84%) as a yellowish-green syrup; [ $\alpha$ ]<sub>D</sub><sup>20</sup> = +131.33 (*c* 0.5, CHCl<sub>3</sub>); IR (KBr): 3432, 2988, 2944, 2836, 1725, 1377, 1211, 1078, 1020 cm<sup>-1</sup>; <sup>1</sup>H NMR (300 MHz, CDCl<sub>3</sub>, 298 K):  $\delta$  6.93 (dd, 1H, *J* = 15.8, 4.9 Hz, C<sub>β</sub>H), 6.11 (dd, 1H, *J* = 15.8, 1.6 Hz, C<sub>α</sub>H), 5.77 (d, 1H, *J* = 3.6 Hz, C<sub>1</sub>H), 4.64 (t, 1H, *J* = 3.9 Hz, C<sub>2</sub>H), 4.49 (ddd, 1H, *J* = 9.1, 4.9, 1.6 Hz, C<sub>4</sub>H), 3.74 (s, 3H, COOMe), 3.46 (s, 3H, OMe), 3.33 (dd, 1H, *J* = 9.1, 4.2 Hz, C<sub>3</sub>H), 1.57 (s, 3H, Me), 1.35 (m, 3H, Me); <sup>13</sup>C NMR (75 MHz, CDCl<sub>3</sub>, 298 K):  $\delta$  166.3, 143.7, 121.8, 113.0, 103.8, 84.6, 76.9, 76.7, 58.4, 51.5, 26.5, 26.2; HRMS (ESI+): *m/z* calculated for C<sub>12</sub>H<sub>18</sub>O<sub>6</sub> [M<sup>+</sup> + Na] 281.1001, found 281.1003.

**Methyl (3R)-3-benzylamino-3-[6-methoxy-2,2-dimethyl-(3aR,6R,6aR)-perhydrofuro[2,3-d][1,3]dioxol-5-yl]propanoate (16) and Methyl (3S)-3-Benzylamino-3-[6-methoxy-2,2-dimethyl-(3aR,6S,6aR)-perhydrofuro[2,3-d][1,3]dioxol-5-yl]propanoate (17)**. A solution of **15** (4.0 g, 15.5 mmol) and benzyl amine (4.2 mL, 38.7 mmol) was stirred at room temperature. After 12 h, the reaction mixture was purified by column chromatography. First eluted (60–120 mesh Silica gel, 10% ethyl acetate in pet. ether) was **17** (0.50 g, 13%) as a pale yellow syrup; [ $\alpha$ ]<sub>D</sub><sup>20</sup> = +146.96 (*c* 0.46, CHCl<sub>3</sub>); IR (KBr): 3453, 2987, 2939, 2834, 1733, 1447, 1375, 1214, 1166, 1085 cm<sup>-1</sup>; <sup>1</sup>H NMR (500 MHz, CDCl<sub>3</sub>, 298 K):  $\delta$  7.30–7.24 (m, 4H, Ar–H), 7.18 (m, 1H, Ar–H) 5.65 (d, 1H, *J* = 3.6 Hz, C<sub>1</sub>H), 4.58 (t, 1H, *J* = 3.7 Hz, C<sub>2</sub>H), 3.92 (dd, 1H, *J* = 8.6, 3.7 Hz, C<sub>4</sub>H), 3.88 (d, 1H, *J* = 12.9 Hz, PhCH<sub>2</sub>), 3.74 (dd, 1H, *J* = 8.6, 3.7 Hz, C<sub>3</sub>H), 3.71 (d, 1H, *J* = 12.9 Hz, PhCH<sub>2</sub>) 3.66 (s, 3H, COOMe), 3.34 (s, 3H, OMe), 3.19 (m, 1H, C<sub>β</sub>H), 2.57 (m, 2H, C<sub>α</sub>H), 1.53 (s, 3H, Me), 1.33

(m, 3H, Me); <sup>13</sup>C NMR (75 MHz, CDCl<sub>3</sub>, 298 K):  $\delta$  172.5, 140.4, 128.3(4C), 127.0, 113.0, 103.9, 80.8, 80.4, 77.4, 58.0, 54.2, 51.6, 51.2, 36.5, 26.8, 26.6; (ESIMS): *m/z* [M<sup>+</sup> + H] calculated for C<sub>19</sub>H<sub>27</sub>NO<sub>6</sub> 365, found 366.

Second eluted (60–120 mesh Silica gel, 20% ethyl acetate in pet. ether) was major diastereomer **16** (3.0 g, 53%) as a pale-yellow syrup; [ $\alpha$ ]<sub>D</sub><sup>20</sup> = +105.25 (*c* 0.2, CHCl<sub>3</sub>); IR (KBr): 3334, 2987, 2935, 2831, 1735, 1494, 1373, 1218, 1167, 1086 cm<sup>-1</sup>; <sup>1</sup>H NMR (300 MHz, CDCl<sub>3</sub>, 298 K)  $\delta$  7.30–7.15 (m, 5H, Ar–H), 5.64 (d, 1H, *J* = 3.6 Hz, C<sub>1</sub>H), 4.60 (t, 1H, *J* = 4.0 Hz, C<sub>2</sub>H), 4.05 (dd, 1H, *J* = 8.8, 4.3 Hz, C<sub>4</sub>H), 3.79 (m, 2H, PhCH<sub>2</sub>), 3.64 (s, 3H, COOMe), 3.60 (dd, 1H, *J* = 8.8, 4.3 Hz, C<sub>3</sub>H), 3.43 (s, 3H, OMe), 3.31 (m, 1H, C<sub>β</sub>H), 2.56 (dd, 1H, *J* = 15.6, 5.1 Hz, C<sub>α</sub>H<sub>(pro-S)</sub>), 2.44 (dd, 1H, *J* = 15.6, 7.5 Hz, C<sub>α</sub>H<sub>(pro-R)</sub>), 1.56 (s, 3H, Me), 1.34 (m, 3H, Me); <sup>13</sup>C NMR (75 MHz, CDCl<sub>3</sub>, 298 K):  $\delta$  172.7, 140.5, 128.3(2C), 128.2(2C), 126.9, 113.1, 103.8, 81.5, 79.5, 77.3, 57.9, 55.0, 51.7, 51.6, 35.8, 26.9, 26.6; (ESIMS): *m/z* [M<sup>+</sup> + H] calculated for C<sub>19</sub>H<sub>27</sub>NO<sub>6</sub> 366.1916, found 366.1930.

**Methyl (3R)-3-[(tert.butoxy)carbonylamino]-3-[6-methoxy-2,2-dimethyl-(3aR,6R,6aR)-perhydrofuro[2,3-d][1,3]dioxol-5-yl]propanoate (3)**. A mixture of **16** (0.95 g, 2.6 mmol) and 10% Pd–C (cat.) in methanol (5 mL) was stirred at room temperature under hydrogen atmosphere for 12 h. The reaction mixture was filtered and filtrate evaporated to give amine **18** as yellow syrup, which was used as such for further reaction.

A solution of the above amine **18** in CH<sub>2</sub>Cl<sub>2</sub> (5 mL) was treated with (Boc)<sub>2</sub>O (0.72 mL, 3.27 mmol) at 0 °C and stirred at room temperature for 2 h. It was treated with water (5 mL) and extracted with CH<sub>2</sub>Cl<sub>2</sub> (2 × 10 mL). Organic layer was washed with brine (5 mL), dried (Na<sub>2</sub>SO<sub>4</sub>), evaporated and the residue purified by column chromatography (60–120 mesh Silica gel, 20% ethyl acetate in pet. ether) to give **3** (0.61 g, 60%) as a pale-yellow syrup; [ $\alpha$ ]<sub>D</sub><sup>20</sup> = +174.6 (*c* 0.6, CHCl<sub>3</sub>); IR (KBr): 3362, 2981, 2935, 1739, 1714, 1507, 1369, 1167, 1023 cm<sup>-1</sup>; <sup>1</sup>H NMR (400 MHz, CDCl<sub>3</sub>, 298 K):  $\delta$  5.71 (d, 1H, *J* = 3.6 Hz, C<sub>1</sub>H), 5.24 (d, 1H, *J* = 8.1 Hz, NH), 4.69 (t, 1H, *J* = 3.9 Hz, C<sub>2</sub>H), 4.10 (m, 1H, C<sub>β</sub>H), 3.96 (t, 1H, *J* = 8.2 Hz, C<sub>4</sub>H), 3.67 (s, 3H, COOMe), 3.61 (dd, 1H, *J* = 8.3, 4.4 Hz, C<sub>3</sub>H), 3.44 (s, 3H, OMe), 2.64 (m, 2H, C<sub>α</sub>H), 1.56 (s, 3H, Me), 1.44 (s, 9H, Boc), 1.35 (m, 3H, Me); <sup>13</sup>C NMR (75 MHz, CDCl<sub>3</sub>, 298 K):  $\delta$  171.5, 155.1, 112.9, 103.5, 83.0, 79.1, 78.5, 77.2, 58.0, 51.6, 49.5, 35.9, 28.3(3C), 26.7, 26.5; HRMS (ESI+): *m/z* calculated for C<sub>17</sub>H<sub>30</sub>NO<sub>8</sub> [M<sup>+</sup> + H] 376.1971, found 376.1982.

**Methyl (3S)-3-[(tert.butoxy)carbonylamino]-3-[6-methoxy-2,2-dimethyl-(3aR,6R,6aR)-perhydrofuro [2,3-d][1,3]dioxol-5-yl]propanoate (20)**. A mixture of **17** (1.0 g, 2.7 mmol) and 10% Pd–C (cat.) in methanol (5 mL) was stirred at room temperature under hydrogen atmosphere for 12 h. The reaction mixture was filtered and evaporated to give amine **19** as a yellow syrup, which was used as such for further reaction.

A solution of the above amine **19** in CH<sub>2</sub>Cl<sub>2</sub> (5 mL) was treated with (Boc)<sub>2</sub>O (0.56 mL, 2.6 mmol) at 0 °C and stirred at room temperature for 2 h. Worked up as described for **3** and purified the residue by column chromatography (60–120 mesh Silica gel, 20% ethyl acetate in pet. ether) to give **20** (0.5 g, 49%) as a pale-yellow syrup; [ $\alpha$ ]<sub>D</sub><sup>20</sup> = +78.88 (*c* 0.1, CHCl<sub>3</sub>); IR (KBr): 3441, 2982, 2938, 1713, 1508, 1373, 1166, 1023 cm<sup>-1</sup>; <sup>1</sup>H NMR (400 MHz, CDCl<sub>3</sub>, 298 K)  $\delta$  5.73 (d, *J* = 3.9 Hz, C<sub>1</sub>H), 4.88 (d, 1H, *J* = 9.7 Hz, NH), 4.66 (t, 1H, *J* = 4.0 Hz, C<sub>2</sub>H), 4.34 (q, 1H, *J* = 7.7 Hz, C<sub>β</sub>H), 4.02 (d, 1H, *J* = 9.2 Hz, C<sub>4</sub>H), 3.67 (s, 3H, COOMe), 3.49 (s, 3H, OMe), 3.45 (dd, 1H, *J* = 7.6, 3.6 Hz, C<sub>3</sub>H), 2.59 (m, 2H, C<sub>α</sub>H), 1.56 (s, 3H, Me), 1.44 (s, 9H, Boc), 1.35 (m, 3H, Me); <sup>13</sup>C NMR (75 MHz, CDCl<sub>3</sub>, 298 K):  $\delta$  171.2, 155.3, 113.2, 104.0, 80.8, 79.6, 79.5, 77.2, 58.7, 51.7, 47.2, 38.4, 28.3(3C), 26.8, 26.5; HRMS (ESI+): *m/z* calculated for C<sub>17</sub>H<sub>29</sub>NO<sub>8</sub> [M<sup>+</sup> + Na] 398.179, found 398.1787.

**(R)-Methyl-3-((3aR,5R,6R,6aR)-6-methoxy-2,2-dimethyl-tetrahydrofuro[2,3-d][1,3]-dioxol-5-yl)-3-((R)-2-methoxy-2-phenylacetamido)propanoate (23)**. A stirred solution of **3** (0.05 g, 0.13 mmol) in dry CH<sub>2</sub>Cl<sub>2</sub> (0.5 mL) at 0 °C under N<sub>2</sub> atmosphere was treated with CF<sub>3</sub>COOH (0.1 mL) at room temperature and stirred for 2 h. The reaction mixture was evaporated and the residue





Boc), 1.37 (d, 3H,  $J = 7.0$  Hz, CH<sub>3</sub>-5); 1.33 (m, 9H, CH<sub>3</sub>-3, 2 × Me), 1.32 (m, 3H, Me), 1.30 (d, 3H,  $J = 7.0$  Hz, CH<sub>3</sub>-1).

**Boc-L-Ala-(R)-β-Caa<sub>(r)</sub>-L-Ala-(R)-β-Caa<sub>(r)</sub>-L-Ala-(R)-β-Caa<sub>(r)</sub>-L-Ala-OMe (9).** A solution of **32** (0.07 g, 0.1 mmol), HOBT (0.02 g, 0.15 mmol) and EDCI (0.02 g, 0.15 mmol) in CH<sub>2</sub>Cl<sub>2</sub> (5 mL) was stirred at 0 °C under a N<sub>2</sub> atmosphere for 15 min, treated sequentially with **31** [prepared from **5** (0.06 g, 0.11 mmol) and CF<sub>3</sub>COOH (0.1 mL) in dry CH<sub>2</sub>Cl<sub>2</sub> (0.5 mL) at 0 °C] and DIPEA (0.04 mL, 0.3 mmol) and stirred for 8 h. Worked up as described for **27** and purified the residue by column chromatography (60–120 mesh Silica gel, 3.5% MeOH in CHCl<sub>3</sub>) to afford **9** (0.04 g, 34%) as a white solid; mp 245 °C;  $[\alpha]_{\text{D}}^{20} = +141.90$  (c 0.1, CHCl<sub>3</sub>); IR (KBr): 3278, 2926, 1635, 1542, 1377, 1229, 1165, 1091, 1026 cm<sup>-1</sup>; <sup>1</sup>H NMR (600 MHz, CD<sub>3</sub>OH, 279 K): δ 8.25 (d, 1H,  $J = 6.0$  Hz, NH-7), 8.18 (d, 1H,  $J = 9.2$  Hz, NH-6), 8.09 (d, 1H,  $J = 8.1$  Hz, NH-3), 8.08 (d, 1H,  $J = 9.2$  Hz, NH-5), 7.96 (d, 1H,  $J = 8.8$  Hz, NH-2), 7.79 (d, 1H,  $J = 9.0$  Hz, NH-4), 6.96 (d, 1H,  $J = 5.8$  Hz, NH-1), 5.77 (d, 1H,  $J = 3.5$  Hz, C<sub>1</sub>H-2), 5.74 (d, 1H,  $J = 3.5$  Hz, C<sub>1</sub>H-4), 5.72 (d, 1H,  $J = 3.5$  Hz, C<sub>1</sub>H-6), 4.77 (t, 1H,  $J = 4.0$  Hz, C<sub>2</sub>H-4), 4.76 (t, 1H,  $J = 4.0$  Hz, C<sub>2</sub>H-2), 4.74 (t, 1H,  $J = 4.0$  Hz, C<sub>2</sub>H-6), 4.56 (m, 1H, C<sub>β</sub>H-2), 4.42 (m, 1H, C<sub>β</sub>H-6), 4.33 (m, 1H, C<sub>β</sub>H-4), 4.37 (m, 1H, C<sub>α</sub>H-7), 4.18 (m, 2H, C<sub>α</sub>H-3, 5), 4.01 (m, 2H, C<sub>α</sub>H-1, C<sub>α</sub>H-4), 3.91 (t, 1H,  $J = 8.4$ , 6.8 Hz, C<sub>4</sub>H-2), 3.82 (t, 1H,  $J = 8.0$  Hz, C<sub>4</sub>H-6), 3.69 (s, 3H, COOMe), 3.62 (m, 3H, C<sub>3</sub>H-2, 4, 6), 3.38 (s, 3H, OMe), 3.35 (s, 6H, 2 × OMe), 2.58 (dd, 1H,  $J = 14.8$ , 2.8 Hz, C<sub>α</sub>H<sub>(pro-S)}</sub>-2), 2.54 (m, 2H, C<sub>α</sub>H<sub>(pro-S)}</sub>-4, 6), 2.51 (m, 1H, C<sub>α</sub>H<sub>(pro-R)}</sub>-4), 2.47 (dd, 1H,  $J = 13.8$ , 8.6 Hz, C<sub>α</sub>H<sub>(pro-R)}</sub>-6), 2.40 (dd, 1H,  $J = 14.8$ , 9.4 Hz, C<sub>α</sub>H<sub>(pro-R)}</sub>-2), 1.50 (s, 3H, Me), 1.47 (s, 3H, Me), 1.46 (s, 12H, Boc, Me), 1.42 (d, 3H,  $J = 7.7$  Hz, CH<sub>3</sub>-5), 1.40 (d, 3H,  $J = 7.4$  Hz, CH<sub>3</sub>-7), 1.42 (m, 3H, Me), 1.33 (m, 3H, CH<sub>3</sub>-3), 1.32 (m, 3H, Me), 1.31 (m, 6H, CH<sub>3</sub>-1, Me);

<sup>1</sup>H NMR (600 MHz, CD<sub>3</sub>CN, 279 K): δ 7.47 (d, 1H,  $J = 9.4$  Hz, NH-6), 7.38 (d, 1H,  $J = 4.5$  Hz, NH-5), 7.31 (d, 1H,  $J = 6.4$  Hz, NH-7), 7.19 (d, 1H,  $J = 9.4$  Hz, NH-4), 7.07 (d, 1H,  $J = 9.2$  Hz, NH-2), 6.86 (d, 1H,  $J = 3.4$  Hz, NH-3), 5.82 (d, 1H,  $J = 5.5$  Hz, NH-1), 5.75 (d, 1H,  $J = 3.5$  Hz, C<sub>1</sub>H-2), 5.73 (d, 1H,  $J = 3.5$  Hz, C<sub>1</sub>H-4), 5.68 (d, 1H,  $J = 3.5$  Hz, C<sub>1</sub>H-6), 4.74 (t, 1H,  $J = 3.8$  Hz, C<sub>2</sub>H-2), 4.72 (t, 1H,  $J = 3.8$  Hz, C<sub>2</sub>H-4), 4.69 (t, 1H,  $J = 3.8$  Hz, C<sub>2</sub>H-6), 4.50 (m, 1H, C<sub>β</sub>H-2), 4.32 (m, 1H, C<sub>β</sub>H-4), 4.30 (m, 1H, C<sub>β</sub>H-6), 4.23 (m, 1H, C<sub>α</sub>H-7), 4.05 (m, 1H, C<sub>α</sub>H-3), 4.00 (m, 1H, C<sub>α</sub>H-5), 3.99 (m, 1H, C<sub>α</sub>H-1), 3.95 (t, 1H,  $J = 7.5$  Hz, C<sub>4</sub>H-4), 3.87 (t, 1H,  $J = 8.2$  Hz, C<sub>4</sub>H-2), 3.80 (t, 1H,  $J = 7.6$  Hz, C<sub>4</sub>H-6), 3.65 (s, 3H, COOMe), 3.60 (dd, 1H,  $J = 8.7$ , 4.5 Hz, C<sub>3</sub>H-6), 3.57 (dd, 1H,  $J = 8.8$ , 4.4 Hz, C<sub>3</sub>H-4), 3.54 (dd, 1H,  $J = 8.8$ , 4.2 Hz, C<sub>3</sub>H-2), 3.33 (s, 6H, 2xOMe), 3.28 (s, 3H, OMe), 2.46 (dd, 1H,  $J = 14.8$ , 2.8 Hz, C<sub>α</sub>H<sub>(pro-S)}</sub>-2), 2.42 (m, 1H, C<sub>α</sub>H<sub>(pro-S)}</sub>-4), 2.49 (m, 1H, C<sub>α</sub>H<sub>(pro-R)}</sub>-4), 2.38 (m, 2H, C<sub>α</sub>H<sub>(pro-R)}</sub>-6, C<sub>α</sub>H<sub>(pro-S)}</sub>-6), 2.32 (dd, 1H,  $J = 14.8$ , 9.4 Hz, C<sub>α</sub>H<sub>(pro-R)}</sub>-2), 1.49 (s, 3H, Me), 1.46 (s, 9H, Boc), 1.44 (s, 6H, 2 × Me), 1.38 (m, 3H,  $J = 7.0$  Hz, CH<sub>3</sub>-5), 1.37 (m, 3H,  $J = 6.3$  Hz, CH<sub>3</sub>-7), 1.31 (m, 6H, CH<sub>3</sub>-3, Me), 1.30 (m, 3H, Me), 1.29 (m, 6H, CH<sub>3</sub>-1, Me); <sup>13</sup>C NMR (150 MHz, CD<sub>3</sub>CN): δ 175.2, 174.6, 174.1, 174.0, 173.3, 172.5, 172.0, 157.2, 113.8, 113.6(2C), 105.4, 105.3(2C), 84.4, 83.6(2C), 80.9, 80.3, 79.7, 79.6, 78.8, 78.7, 78.4, 58.4, 58.3, 58.2, 53.1, 53.0, 52.6(2C), 51.2, 50.0(2C), 49.9, 39.5, 39.2, 39.0, 29.1(3C), 27.6, 27.5, 27.4, 27.3, 27.2, 27.1, 18.5(2C), 18.0, 17.7; HRMS (ESI+):  $m/z$  [M<sup>+</sup> + Na] calculated for C<sub>51</sub>H<sub>83</sub>N<sub>7</sub>O<sub>22</sub> 1168.5488, found 1168.5460.

## ■ ASSOCIATED CONTENT

### Supporting Information

Experimental details of several compounds, NMR spectra, solvent titration plots, distance constraints used in MD calculations. This material is available free of charge via the Internet at <http://pubs.acs.org>.

## ■ AUTHOR INFORMATION

### Corresponding Author

\*esmvee@iict.res.in; kunwar@iict.res.in

### Author Contributions

‡These authors contributed equally to this work

## Notes

The authors declare no competing financial interest.

## ■ ACKNOWLEDGMENTS

We are thankful for financial support from MLP-0010 of CSIR, New Delhi. T.A.Y. and M.C. are thankful to CSIR, New Delhi for the financial support in the form of fellowship.

## ■ DEDICATION

Dedicated to Dr. J. S. Yadav on the occasion of his 62nd birthday.

## ■ REFERENCES

- (1) (a) Hill, D. J.; Mio, M. J.; Prince, R. B.; Hughes, T. S.; Moore, J. S. *Chem. Rev.* **2001**, *101*, 3893–4011. (b) Hintermann, T.; Gademann, K.; Jaun, B.; Seebach, D. *Helv. Chim. Acta* **1998**, *81*, 983–1002. (c) Hanessian, S.; Luo, X.; Schaum, R.; Michnick, S. *J. Am. Chem. Soc.* **1998**, *120*, 8569–8570. (d) Long, D. D.; Hungerford, N. L.; Smith, M. D.; Brittain, D. E. A.; Marquess, D. G.; Claridge, T. D. W.; Fleet, G. W. *J. Tetrahedron Lett.* **1999**, *40*, 2195–2198.
- (2) (a) Seebach, D.; Matthews, J. L. *Chem. Commun.* **1997**, 2015–2022. (b) Gellman, S. H. *Acc. Chem. Res.* **1998**, *31*, 173–180. (c) Kirschenbaum, K.; Zuckerman, R. N.; Dill, D. A. *Curr. Opin. Struct. Biol.* **1999**, *9*, 530–535. (d) Stigers, K. D.; Soth, M. J.; Nowick, J. S. *Curr. Opin. Chem. Biol.* **1999**, *3*, 714–723. (e) Smith, M. D.; Fleet, G. W. *J. Pept. Sci.* **1999**, *5*, 425–441. (f) Cheng, R. P.; Gellman, S. H.; De Grado, W. F. *Chem. Rev.* **2001**, *101*, 3219–3232. (g) Venkatraman, J.; Shankaramma, S. C.; Balam, P. *Chem. Rev.* **2001**, *101*, 3131–3152. (h) Cubberley, M. S.; Iverson, B. L. *Curr. Opin. Chem. Biol.* **2001**, *5*, 650–653. (i) Fulop, F. *Chem. Rev.* **2001**, *101*, 2181–2204. (j) Seebach, D.; Hook, D. F.; Glatli, A. *Biopolymer* **2005**, *84*, 23–37. (k) Martinek, T. A.; Füllöp, F. *Eur. J. Biochem.* **2003**, *270*, 3657–3666. (l) Rathore, N.; Gellman, S. H.; de Pablo, J. J. *Biophys. J.* **2006**, *91*, 3425–3435. (m) Goodman, C. M.; Choi, S.; Shandler, S.; DeGrado, W. F. *Nature Chem. Biol.* **2007**, *3*, 252–262. (n) Hecht, S., Huc, I., Eds. *Foldamers: Structure, Properties and Applications*; Wiley-VCH: Weinheim, Germany, 2007. (o) Saraogi, I.; Hamilton, A. D. *Chem. Soc. Rev.* **2009**, *38*, 1726–1743. (q) Guichard, G.; Huc, I. *Chem. Commun.* **2011**, 5933–5941. (p) Vasudev, P. G.; Chatterjee, S.; Shamala, N.; Balam, P. *Chem. Rev.* **2011**, *111*, 657–687. (q) Boullière, F.; Thétiot-Laurent, S.; Kouklovsky, C.; Alezra, V. *Amino Acids* **2011**, *41*, 687–707. (r) Martinek, T. A.; Fulop, F. *Chem. Soc. Rev.* **2012**, *41*, 687–702.
- (3) (a) Seebach, D.; Beck, A. K.; Bierbaum, D. J. *Chem. Biodiversity* **2004**, *1*, 1111–1239. (b) Karle, I. L.; Gopi, H. N.; Balam, P. *Proc. Natl. Acad. Sci. U.S.A.* **2001**, *98*, 3716–3719. (c) Gopi, H. N.; Roy, R. S.; Raghothama, S. R.; Karle, I. L.; Balam, P. *Helv. Chim. Acta* **2002**, *85*, 3313–3330. (d) Roy, R. S.; Balam, P. *J. Peptide Res.* **2004**, *63*, 279–289.
- (4) (a) Horne, W. S.; Gellman, S. H. *Acc. Chem. Res.* **2008**, *41*, 1399–1408. (b) Pils, L. K. A.; Reiser, O. *Amino Acids* **2011**, *41*, 709–718.
- (5) (a) Hayen, A.; Schmitt, M. A.; Nagassa, N.; Thomson, K. A.; Gellman, S. H. *Angew. Chem., Int. Ed.* **2004**, *43*, 505–510. (b) De Pol, S.; Zorn, C.; Klein, C. D.; Zerbe, O.; Reiser, O. *Angew. Chem., Int. Ed.* **2004**, *43*, 511–514.
- (6) Bolin, A. K.; Millhauser, G. L. *Acc. Chem. Res.* **1999**, *32*, 1027–1033 and references cited therein.
- (7) Jagadeesh, B.; Prabhakar, A.; Sharma, G. D.; Chandrasekhar, S.; Chandrashekar, G.; Reddy, M. S.; Jagannadh, B. *Chem. Commun.* **2007**, 371–373.
- (8) (a) Schmitt, M. A.; Choi, S. H.; Guzei, I. A.; Gellman, S. H. *J. Am. Chem. Soc.* **2005**, *127*, 13130–13131. (b) Choi, S. H.; Guzei, I. A.; Gellman, S. H. *J. Am. Chem. Soc.* **2007**, *129*, 13780–13781. (c) Choi, S. H.; Guzei, I. A.; Gellman, S. H. *J. Am. Chem. Soc.* **2008**, *130*, 6544–6550. (d) Schmitt, M. A.; Choi, S. H.; Guzei, I. A.; Gellman, S. H. *J. Am. Chem. Soc.* **2006**, *128*, 4538–4539.
- (9) Seebach, D.; Jaun, B.; Sebesta, R.; Mathad, R. I.; Flogel, O.; Limbach, M. *Helv. Chim. Acta* **2006**, *89*, 1801–1825.

- (10) (a) Sadowsky, J. D.; Schmitt, M. A.; Lee, H. S.; Umezawa, N.; Wang, S.; Tomita, Y.; Gellman, S. H. *J. Am. Chem. Soc.* **2005**, *127*, 11966–11968. (b) Sadowsky, J. D.; Fairlie, W. D.; Hadley, E. B.; Lee, H. S.; Umezawa, N.; Nikolovska-Coleska, Z.; Wang, S.; Huang, D. C. S.; Tomita, Y.; Gellman, S. H. *J. Am. Chem. Soc.* **2007**, *129*, 139–154.
- (11) Sharma, G. V. M.; Chandramouli, N.; Choudhary, M.; Nagendar, P.; Ramakrishna, K. V. S.; Kunwar, A. C.; Schramm, P.; Hofmann, H.-J. *J. Am. Chem. Soc.* **2009**, *131*, 17335–17344.
- (12) (a) Sharma, G. V. M.; Reddy, K. R.; Krishna, P. R.; Sankar, A. R.; Narsimulu, K.; Kumar, S. K.; Jayaprakash, P.; Jagannadh, B.; Kunwar, A. C. *J. Am. Chem. Soc.* **2003**, *125*, 13670–13671. (b) Sharma, G. V. M.; Reddy, K. R.; Krishna, P. R.; Sankar, A. R.; Jayaprakash, P.; Jagannadh, B.; Kunwar, A. C. *Angew. Chem., Int. Ed.* **2004**, *43*, 3961–3965. (c) Sharma, G. V. M.; Jadhav, V. B.; Madavi, C.; Ramakrishna, K. V. S.; Jayaprakash, P.; Narsimulu, K.; Subash, V.; Kunwar, A. C. *J. Am. Chem. Soc.* **2006**, *128*, 14657–668. (d) Sharma, G. V. M.; Manohar, V.; Dutta, S. K.; Subash, V.; Kunwar, A. C. *J. Org. Chem.* **2008**, *73*, 3689–3698. (e) Sharma, G. V. M.; Shoban Babu, B.; Chatterjee, D.; Ramakrishna, K. V. S.; Kunwar, A. C.; Schramm, P.; Hofmann, H.-J. *J. Org. Chem.* **2009**, *74*, 6703–6713. (f) Sharma, G. V. M.; Shoban Babu, B.; Ramakrishna, K. V. S.; Nagendar, P.; Kunwar, A. C.; Schramm, P.; Baldauf, C.; Hofmann, H.-J. *Chem.—Eur. J.* **2009**, *15*, 5552–5566.
- (13) Sharma, G. V. M.; Goverdhan Reddy, V.; Subhash Chander, A.; Ravinder Reddy, K. *Tetrahedron Asymmetry* **2002**, *13*, 21–24.
- (14) Barrett, A. G.; Lebold, S. J. *Org. Chem.* **1991**, *56*, 4875–4884.
- (15) (a) Sharma, G. V. M.; Nagendar, P.; Jayaprakash, P.; Krishna, P. R.; Ramakrishna, K. V. S.; Kunwar, A. C. *Angew. Chem., Int. Ed.* **2005**, *44*, 5878–5882. (b) Srinivasulu, G.; Kumar, S. K.; Sharma, G. V. M.; Kunwar, A. C. *J. Org. Chem.* **2006**, *71*, 8395–8400.
- (16) (a) Baldauf, C.; Günther, R.; Hofmann, H.-J. *Biopolymers* **2006**, *84*, 408–413. (b) Zhu, X.; Yethiraj, A.; Cui, Q. *Theory Comput.* **2007**, *3*, 1538–1549.
- (17) (a) Tomasini, C.; Luppi, G.; Magda, M. J. *J. Am. Chem. Soc.* **2006**, *128*, 2410–2420. (b) Motorina, I. A.; Huel, C.; Quiniou, E.; Mispelter, J.; Adjadj, E.; Grierson, D. S. *J. Am. Chem. Soc.* **2001**, *123*, 8–17. (c) Duddy, W. J.; Nissink, J. W. M.; Allen, F. H.; Milner-White, E. J. *Protein Sci.* **2004**, *13*, 3051–3055. (d) Song, B.; Kibler, P.; Malde, A.; Kodukula, K.; Galande, A. K. *J. Am. Chem. Soc.* **2010**, *132*, 4508–4509. (e) Song, B.; Kibler, P.; Malde, A.; Kodukula, K.; Galande, A. K. *J. Am. Chem. Soc.* **2010**, *132*, 4508–4509. (f) Song, B.; Bomar, M. G.; Kibler, P.; Malde, A.; Kodukula, K.; Galande, A. K. *Org. Lett.* **2012**, *14*, 732–735.
- (18) Sharma, G. V. M.; Reddy, K. S.; Basha, S. J.; Reddy, K. R.; Sarma, A. V. S. *Organic. Biomol. Chem.* **2011**, *9*, 8102–8111.
- (19) (a) Sharma, G. V. M.; Reddy, P. S.; Chatterjee, D.; Kunwar, A. C. *J. Org. Chem.* **2011**, *76*, 1562–1571. (b) Sharma, G. V. M.; Reddy, P. S.; Chatterjee, D.; Kunwar, A. C. *Tetrahedron* **2012**, *68*, 4390–4398.
- (20) (a) Sharma, G. V. M.; Nagendar, P.; Ramakrishna, K. V. S.; Chandramouli, N.; Choudhary, M.; Kunwar, A. C. *Chem. Asian J.* **2008**, *3*, 969–983. (b) Sharma, G. V. M.; Chandramouli, N.; Basha, S. J.; Nagendar, P.; Ramakrishna, K. V. S.; Sarma, A. V. S. *Chem. Asian J.* **2011**, *6*, 84–97.
- (21) (a) Chan, L. C.; Cox, G. B. *J. Org. Chem.* **2007**, *72*, 8863–8869. (b) Bodanszky, M. *Peptide Chemistry: A Practical Textbook*; Springer: New York, 1988.
- (22) Crich, D.; Neelamkavil, S. *Tetrahedron* **1997**, *43*, 3095–3108.
- (23) (a) Shimona, F.; Kusaka, H.; Wada, K.; Azami, H.; Yasunami, M.; Suzuki, T.; Hagiwara, H.; Ando, M. *J. Org. Chem.* **1998**, *63*, 920–929. (b) Seco, J. S.; Quio, E.; Riguera, R. *Chem. Rev.* **2004**, *104*, 17–117.
- (24) See Supporting Information.
- (25) Solvent titration studies were carried out by sequentially adding up to 33% (v/v) of DMSO-*d*<sub>6</sub> to 600  $\mu$ L CDCl<sub>3</sub> solutions of the peptides.
- (26) Creighton, T. E. *Proteins: Structures and Molecular Properties*, 2nd ed.; W. H. Freeman and Company: New York, 1993.
- (27) Schmitt, M. A.; Weisblum, B.; Gellman, S. H. *J. Am. Chem. Soc.* **2007**, *129*, 417–428.
- (28) Glättli, A.; Daura, X.; Seebach, D.; van Gunsteren, W. F. *J. Am. Chem. Soc.* **2002**, *124*, 12972–12978.
- (29) (a) States, D. J.; Haberkorn, R. A.; Ruben, D. J. *J. Magn. Reson.* **1982**, *48*, 286–292. (b) Marion, D.; Ikura, M.; Tschudin, R.; Bax, A. D. *J. Magn. Reson.* **1989**, *85*, 393–399.